

# Restricted Perceptions, Regime Switches and the Effective Lower Bound \*

([Link to Latest Version](#))

Tolga Ozden<sup>†</sup> Rafael Wouters<sup>‡</sup>

October 30, 2020

## Abstract

We analyze the business cycle implications of adaptive learning at the effective lower bound (ELB). Regime shifts by monetary policy are not directly observed by agents, and instead they gradually learn about the changes based on past observations. We first derive the stability conditions associated with these models in a general regime-switching framework, and then estimate the Smets-Wouters (2007) model on U.S. data over the period 1966-2016 under a variety of learning rules, where agents do not immediately recognize the break in the monetary policy regime when the ELB on nominal interest rates starts binding. Our results show that, (i) AL models typically outperform the regime-switching RE model in terms of in-sample fit, (ii) the impulse responses in both RE and learning models change in the same direction with the switch to the ELB episode, but the magnitudes under learning models tend to be smaller, (iii) counterfactual experiments suggest that stronger learning dynamics typically prolong the ELB duration.

*JEL Classification:* E37; E65; C11; C32 .

*Keywords:* Adaptive Learning; Markov-Switching; Effective Lower Bound.

---

\*The research project is funded by the National Bank of Belgium under *the Research Program for Young Researchers*. The views expressed in this paper are those of the authors and do not necessarily reflect the views of the National Bank of Belgium, De Nederlandsche Bank or any other institution to which the authors are affiliated. Earlier versions of the paper have been presented at the QED Workshop at Nova Business School, 10-11 May 2019; EcoMod Conference at the University of Azores, 10-12 July; WEHIA Bank of England Policy Session at City University London, 24-26 June 2019; Barcelona GSE Summer Forum, 20-22 June 2019; lunch seminars at Bank of England, Bank of Canada and University of Amsterdam; and EEA 2020 Virtual.

<sup>†</sup>T.ozden@uva.nl, University of Amsterdam & De Nederlandsche Bank

<sup>‡</sup>Rafael.wouters@nbb.be, National Bank of Belgium

# 1 Introduction

With the onset of the Global Financial Crisis in 2007-08 and the subsequent drop of interest rates to near-zero levels among the leading central banks, there has been increased interest among policymakers and central bankers alike about the effective lower bound (ELB) constraint on nominal interest rates. There is still ongoing debate about the precise impact of the ELB constraint on the economy as a whole and in particular about its macroeconomic cost in terms of aggregate output levels. A common approach in most macroeconomic models examining the ELB episode is the assumption of Rational Expectations Equilibria (REE), where agents have perfect information about the underlying economic conditions along with all other cross-correlations of the relevant macroeconomic variables. In this paper, we contribute to the growing literature on analyzing the effects of ELB episodes by relaxing the perfect information assumption, and instead estimating DSGE models under adaptive learning subject to the ELB constraint.

We model the ELB constraint as a regime shift in monetary policy, which is captured as a Markov-switching process. In this sense, monetary policy follows a standard Taylor rule during normal times as long as the ELB constraint does not bind. When the ELB constraint starts binding, monetary policy switches to a pegged interest rate regime, where it is unable to react to changes in inflation and output gap. This approach is combined with adaptive learning on private sector agents' expectation formation process, which relaxes the assumption that agents have perfect knowledge about the underlying economic conditions. Instead, they have their own forecasting models, possibly under- or over-parameterized, which may not coincide with the correct economic structure. In this sense, agents act as econometricians and update their models each period as new observations become available.

The presence of adaptive learning means that private sector agents use a class of econometric models, where they gradually become aware of the underlying regime switches only to the extent that these switches have an observable impact on their information set. In the context of the ELB, this corresponds to three key deviations from the REE framework: first, as the nominal rates drop to near zero levels following the GFC, agents do not initially know where the lower bound is, and particularly whether and how far the rates will drop into the negative territory. This deviation can also be interpreted as a situation where the lower bound is known to the central bank but unknown to agents, who instead employ a "stochastic lower bound" along the lines of [Masolo & Winant \(2019\)](#). Second, agents do not immediately know the structural changes implied by the regime switch but only learn about them over time, in particular about the cross-correlations and the transmission of shocks. Third and most importantly, the expected duration of the ELB regime is unknown to agents. Studying the business cycle dynamics in this framework is of particular interest, because the underlying shock transmission channels

and the related policy implications are different under adaptive learning compared to the REE framework, as we discuss further below.

The standard RE models come equipped with a perfect foresight assumption about regime switches, which equates the objective expected durations of the underlying regimes with agents' subjective expectations. This typically leads to short periods of anticipated ELB episodes: DSGE models estimated on the U.S. economy report estimates of the expected ELB duration over 2009-2016 ranging between 3 to 9 quarters,<sup>1</sup> whereas the empirical duration was 28 quarters. The difficulty to generate plausibly long ELB durations may be seen as a shortcoming of RE models as it imposes a form of non-rationality on the agents: since, in a given period, they expect to leave the ELB regime soon, they are constantly surprised during the 28 quarter period without ever revising their belief models for an extend period. Our paper makes this non-rationality explicit with the introduction of learning, which allows us to generate more realistic ELB durations that can match the data.

Since there is scant research on misspecified expectations and adaptive learning in regime switching environments, we start with an introductory example using a 1-dimensional Markov-switching model of the Fisher equation and study it under adaptive learning. In this *limited information* framework, we derive the corresponding equilibrium and expectational stability (E-stability) conditions.<sup>2</sup> Of particular interest is the result that the model as a whole remains E-stable even if one of the underlying regimes is E-unstable, as long as this regime is sufficiently short-lived. We call this the *Long run E-stability* principle, in parallel to the *Long-run Determinacy* of [Davig & Leeper \(2007\)](#) used in Markov-switching RE models. We then illustrate this concept in a skeleton version of the baseline New Keynesian model, where the pegged interest rate rule during the ELB regime leads to indeterminacy in a REE setup, and E-unstability in the adaptive learning framework. In both cases, ensuring that ELB durations are short-lived or that the Taylor rule during normal regimes is sufficiently strong, is enough to ensure overall stability.

After studying the theoretical properties of this modeling framework, we introduce a variant of the [Kim & Nelson \(1999\)](#) filter to estimate the class of Markov-switching DSGE models under adaptive learning, both with exogenous and endogenous regime switching. Applying the filter for the Bayesian estimation of the Smets-Wouters ([2007](#)) model yields the following results: the adaptive learning models with regime switching in the monetary policy rule typically outperform the standard RE model (with or without switching in the policy rule) in terms of marginal likelihood under a variety of learning rules. More importantly, we observe systematic differences in the impulse response and shock propagation structure of the models under consideration. In

---

<sup>1</sup>See e.g. [Lindé et al. \(2017\)](#); [Ji & Xiao \(2016\)](#); [Chen \(2017\)](#), among others.

<sup>2</sup>E-stability refers to the stability of model dynamics under adaptive learning. When the stability conditions hold, the learning dynamics converge to an ergodic distribution around the underlying equilibrium, whereas a violation of E-stability conditions results in divergent and explosive learning dynamics.

particular, we find that impulse responses move in the same direction under learning and RE when the economy switches from the normal to the ELB regime, but the magnitudes of change under learning models tend to be smaller. This suggests that REE models may overestimate the impact of the ELB on shock propagation. A side-effect of this result is that REE models may exaggerate the size of fiscal multipliers over this period.

We also consider a number of counterfactual experiments to discuss the effects of learning over the ELB period. We find that simulations under learning typically result in ELB durations longer than the empirical duration of 7 years for the U.S. economy, with values of average inflation and output growth lower than their empirical counterparts. We observe a positive correlation between the ELB duration and the speed of learning (i.e. the constant gain coefficient), where stronger learning dynamics increase the probability of prolonged ELB durations and deflationary spirals. This result emphasizes the importance of keeping private sector expectations anchored through unconventional policy measures such as forward guidance.

The paper is organized as follows: Section 2 illustrates the main concepts in a simple Fisher equation framework with one-forward looking variable. Section 3 provides the general higher dimensional setup, the estimation methodology and the learning rules that we use in our empirical exercise. Section 4 discusses the estimation results for Smets-Wouters (2007) model with both exogenous and endogenous switching. Section 4.6 discusses the stability dynamics and some counterfactual experiments with the learning models. Finally, Section 5 concludes.

## Related Literature

Various approaches have been used in the literature to model the ELB constraint. Some researchers use a perfect foresight & endogenous duration approach, which allows for a joint determination of expectations and regime switches; see e.g. [Maih \(2015\)](#); [Lindé et al. \(2016, 2017\)](#); [Kulish et al. \(2017\)](#). Another method which is more common in VAR-literature is to use a threshold-switching method, where the economy is assumed to be in the ELB regime if interest rates fall below some pre-specified level, see e.g. [Bonam et al. \(2017\)](#). A final approach is to use a Markov-switching framework, where the presence of the ELB regime is determined by its predictive density, see e.g. [Binning & Maih \(2016\)](#). [Lindé et al. \(2017\)](#) show that Markov-switching and endogenous duration approaches typically lead to similar results as long as the ELB constraint is accounted for. In this paper, we use the Markov-switching (MS) approach to model the ELB constraint.<sup>3</sup>

---

<sup>3</sup> Aside from the ELB episode, MS approach recently gained popularity in DSGE literature to model structural changes such as monetary policy switches or volatility breaks, see e.g. [Sims & Zha \(2006\)](#), [David & Leeper \(2007\)](#), [Sims et al. \(2008\)](#), [Liu et al. \(2011\)](#), [Liu & Mumtaz \(2011\)](#), [Bianchi \(2016\)](#), [Bianchi & Ilut \(2017\)](#) and [Bianchi & Melosi \(2017\)](#) for some of the recent work. Other related work includes [Bullard & Duffy \(2004\)](#) that studies learning about unanticipated structural change in productivity in an RBC framework, and [Hollmayr & Matthes \(2015\)](#) that studies consequences of fiscal policy shifts when agents have uncertainty about the switch.

In parallel to this, there is a vast and growing literature on the empirical validation of adaptive learning in DSGE models, as well as monetary and fiscal policy implications of adaptive learning, see [Evans & Honkapohja \(2012\)](#) for a textbook treatment and [Woodford \(2013\)](#) for a comprehensive review of the more recent work. Much of the earlier literature on adaptive learning focused on the learnability of Rational Expectations Equilibria and MSV-learning, focusing on small and temporary deviations from perfect foresight models. [Milani \(2007\)](#) and [Eusepi & Preston \(2011\)](#) are earlier examples of expectations-driven business cycles and how MSV-learning can improve the empirical properties of small-scale DSGE models, while [Bullard & Mitra \(2002\)](#) and [Bullard & Eusepi \(2014\)](#) examine monetary policy implications of this type of learning.

In more recent work, [Slobodyan & Wouters \(2012a\)](#) and [Slobodyan & Wouters \(2012b\)](#) show that further deviations from perfect foresight models with the use of small forecasting rules can lead to further improvements in the fit of a medium-scale DSGE model. On a similar vein, [Quaghebeur \(2018\)](#) examines fiscal policy implications of a VAR-type adaptive learning rule and finds that government spending multipliers are larger under adaptive learning. [Evans et al. \(2008\)](#) and [Evans & Honkapohja \(2010\)](#) examine the implications of adaptive learning for fiscal policy.

While Markov-switching and adaptive learning have both been increasingly popular classes of time-varying DSGE models in recent years, there is little work on DSGE models that consider a combination of both approaches. Closely related theoretical work includes [Branch et al. \(2013\)](#) that studies the properties of MSV-learning in Markov-switching models where agents are informed about regime switches but learn the remaining economic parameters; and [Airaudo & Hajdini \(2019\)](#) that studies equilibria in a Markov-switching framework where agents use an optimal AR(1) rule without accounting for regime switches. Empirical studies closely related to our work include [Gust et al. \(2018\)](#) that examines the ELB episode and forward guidance in a Markov-switching setup under Bayesian learning, where agents are aware of regime switches but have to infer about the underlying regime of the economy; and [Lansing \(2018\)](#) that analyzes the ELB episode in a calibrated setup under adaptive learning where regime switches are unobserved. Our key difference from these empirical papers and one of our key contributions is to extend their framework to non-rational beliefs, and to estimate the resulting DSGE models during the ELB episode.

[Farmer et al. \(2009, 2011\)](#) explore a class of Rational Expectations Equilibria (REE) in Markov-switching models. Since we assume that regimes are never observed, an equilibrium concept in our framework does not coincide with a Rational Expectations Equilibrium in the sense of [Farmer et al. \(2011\)](#). Instead, our approach is a *Restricted Perceptions Equilibrium* (RPE), where agents' model misspecification permanently keep the economy away from the underlying REE.

## 2 Preliminaries

### 2.1 Fisher Equation and Long-run E-stability

In this section, we discuss and clarify some dynamic properties and stability conditions that apply to our modelling approach. We start with a minimal setup that establishes the connection to the previous literature and allows for an analytical discussion of the problems. We then apply the concepts to the more general setup that is applied in the rest of the paper. Consider first a simple model of Fisherian inflation determination without regime switching:

$$\begin{cases} i_t = E_t \pi_{t+1} + r_t, \\ r_t = \rho r_{t-1} + v_t, \\ i_t = \alpha \pi_t, \end{cases} \quad (2.1)$$

where  $r_t$  is the exogenous AR(1) ex-ante real interest rate,  $i_t$  is the nominal interest rate,  $\pi_t$  is inflation, and  $v_t$  is an IID shock process. We assume that monetary policy follows a simple rule by adjusting nominal interest rate to inflation, denoted by  $\alpha$ .<sup>4</sup> After eliminating nominal interest rate  $i_t$ , the system can be re-written as:

$$\begin{cases} \pi_t = \frac{1}{\alpha} (E_t \pi_{t+1} + r_t), \\ r_t = \rho r_{t-1} + v_t. \end{cases} \quad (2.2)$$

We use this small setup as our starting point as it has been extensively analyzed in [Davig & Leeper \(2007\)](#), which is one of the first studies on expectations in a regime switching setup; as well as in [Airaudo & Hajdini \(2019\)](#), which is the first study on small forecasting rules in a regime switching setup. The standard Minimum State Variable (MSV) REE solution takes the form of:

$$\pi_t = d r_t. \quad (2.3)$$

In terms of adaptive learning terminology, (2.3) is known as the the *Perceived Law of Motion* (PLM). The Rational Expectations Equilibrium (REE) value of  $d$  is pinned down by iterating the PLM forward to obtain the one-step ahead expectations, plugging the expectations back into the actual law of motion (2.2) and computing the associated fixed point, which yields  $d = \frac{1}{\alpha - \rho}$ . Hence the law of motion under REE is given by  $\pi_t = \frac{1}{\alpha - \rho} r_t$ . In this benchmark case, the equilibrium is determinate if  $\alpha > 1$ , i.e. if monetary policy is sufficiently aggressive.

[Davig & Leeper \(2007\)](#) consider scenarios where the interest rate reaction parameter  $\alpha$  is subject to exogenous regime switches. Focusing on a two regime environment, assume that  $\alpha$  changes

---

<sup>4</sup>For the remainder, we assume that  $\text{Var}[r_t] = 1$  to simplify the exposure.

stochastically between two regimes,  $s_t = \{1, 2\}$  subject to the transition matrix:

$$Q = \begin{pmatrix} p_{11} & 1 - p_{11} \\ 1 - p_{22} & p_{22} \end{pmatrix}.$$

Then inflation dynamics are given as:

$$\begin{cases} \pi_t = \frac{1}{\alpha(s_t)}(E_t\pi_{t+1} + r_t), \\ r_t = \rho r_{t-1} + v_t, \end{cases} \quad (2.4)$$

with  $\alpha(s_t = 1) = \alpha_1$  and  $\alpha(s_t = 2) = \alpha_2$  denoting the regime-specific parameters. Using  $\pi_{i,t} = \pi_t(s_t = i)$ , we can rewrite the model in a multivariate form:

$$\begin{bmatrix} \alpha_1 & 0 \\ 0 & \alpha_2 \end{bmatrix} \begin{bmatrix} \pi_{1,t} \\ \pi_{2,t} \end{bmatrix} = \begin{bmatrix} p_{11} & p_{12} \\ p_{21} & p_{22} \end{bmatrix} \begin{bmatrix} E_t\pi_{1,t+1} \\ E_t\pi_{2,t+1} \end{bmatrix} + \begin{bmatrix} r_t \\ r_t \end{bmatrix}. \quad (2.5)$$

In a REE framework, the presence of regime switches and the corresponding transition matrix  $Q$  is known to agents. Denoting by  $d_i$  the regime-specific REE solutions, the corresponding regime-dependent 1-step ahead expectations are given by:

$$\begin{cases} E_t[\pi_{t+1}|s_t = 1] = (p_{11}d_1 + p_{12}d_2)\rho r_t, \\ E_t[\pi_{t+1}|s_t = 2] = (p_{21}d_1 + p_{22}d_2)\rho r_t. \end{cases}$$

In other words, agents hold two distinct laws of motion associated with each regime, and they correctly form their expectations after observing the current regime  $s_t$ . [Davig & Leeper \(2007\)](#) show that, in this setup, the equilibrium is determinate as long as the *long-run Taylor principle (LRTP)* is satisfied:<sup>5</sup>

$$\alpha_1\alpha_2 > 1 - ((1 - \alpha_2)p_{11} + (1 - \alpha_1)p_{22}). \quad (2.6)$$

A key insight of this principle is that, the long-run dynamics of the model are determinate even if one of the underlying regimes is indeterminate, provided there is at least one regime that is sufficiently determinate or the probability of entering into the indeterminate regime is sufficiently small. In what follows, we first relax the assumption of full information to replace it with that of learning, and then we extend the long-run determinacy insight into the concept of learnability, i.e. *E-stability* of equilibria.

Our main deviation from the REE framework is that agents do not directly observe or take into account the regime shifts that occur in the economy when forming their expectations. Instead, they hold period-specific expectations that are updated each period as new observations

---

<sup>5</sup>See Appendix A for further details on the derivation of this condition.

become available. Regime switches are unknown to agents ex-ante, and only affect agents' expectations ex-post after new observations become available.

Before introducing adaptive learning, it is useful to first study the equilibrium properties of this setup and compare it with the REE counterpart. Assume that the economy evolves according to (2.4) with two monetary policy regimes, where agents do no observe the regime switches. Their regime-independent PLM and 1-step ahead expectations are given as follows:

$$\pi_t = dr_t \Rightarrow E_t \pi_{t+1} = dE_t r_{t+1} = d\rho r_t, \quad (2.7)$$

where  $d$  denotes the agents' perceived coefficient. The implied Actual Law of Motion (ALM) is then given by:

$$\begin{cases} \pi_t = \frac{1}{\alpha(s_t)}(d\rho + 1)r_t, \\ r_t = \rho r_{t-1} + v_t. \end{cases} \quad (2.8)$$

The assumed form of PLM here does not nest the regime-dependent REE solution. Therefore, any resulting notion of equilibrium under this scenario cannot coincide with the full-information REE. Instead, we refer to the resulting equilibrium as a Restricted Perceptions Equilibrium (RPE), where agents use a restricted and misspecified information set when forming their expectations.<sup>6,7</sup>

In order to identify an RPE, we follow [Hommes & Zhu \(2014\)](#) and impose a moment consistency requirement on the model to pin down the value of  $d$  associated with the equilibrium: the coefficient  $d$  determines the *perceived correlation* between inflation and real rate of interest in agents' PLM, i.e.  $d = \frac{E[\pi_t r_t]}{E[r_t r_t]}$ . In an RPE, the unconditional correlation  $\frac{E[\pi_t r_t]}{E[r_t r_t]}$  implied by the ALM is equal to  $d$ . In other words, agents' forecasting rule is consistent with the actual outcomes on average, but it is misspecified along each regime. The associated unconditional moment in our example is given as:

$$\frac{E[\pi_t r_t]}{E[r_t r_t]} = E\left[\frac{1}{\alpha(s_t)}d\rho + \frac{1}{\alpha(s_t)}\right], \quad (2.9)$$

which involves the long-run distribution (i.e. ergodic distribution) of the Markov chain denoted by  $P$ . Given the transition matrix  $Q$ , this follows  $P = [\frac{1-p_{22}}{2-p_{11}-p_{22}}, \frac{1-p_{11}}{2-p_{11}-p_{22}}]$ .<sup>8</sup> Then the

<sup>6</sup>See ([Evans & Honkapohja, 2012](#)) for an overview of Restricted Perceptions Equilibria in the adaptive learning literature.

<sup>7</sup>In this section we limit our attention to a misspecification related to regime-switches only, while the PLM is otherwise correctly specified. In our empirical exercises, we also allow for misspecification in the forecasting rule. See [Airaudo & Hajdini \(2019\)](#) for theoretical properties of such an example, where two types of misspecification are combined with an AR(1) forecasting rule.

<sup>8</sup>Note that the ergodic distribution is obtained by solving  $P'Q = P$ .

underlying RPE coefficient, which we denote as  $d^{RPE}$ , is given by:<sup>9</sup>

$$d^{RPE} = \frac{\alpha_1(1 - p_{22}) + \alpha_2(1 - p_{11})}{\alpha_1\alpha_2(2 - p_{11} - p_{22}) - \rho\alpha_1(1 - p_{22}) - \rho\alpha_2(1 - p_{11})}. \quad (2.10)$$

Further note that, the regime-specific REE solutions (i.e. the solution when the economy is always in regime  $i$ ) are given by  $d_i = \frac{1}{\alpha_i - \rho}$ ,  $i \in \{1, 2\}$ . In this special case, the underlying RPE is essentially a weighted average of the regime-specific equilibria, where the weights are determined by the long-run distribution of the regimes. Instead of the standard determinacy condition of REE models, our main concept of interest in this case is E-stability.<sup>10</sup> The E-stability principle determines whether the agents can learn an equilibrium around the fixed-point  $d^{RPE-consistent}$  by starting from an arbitrary point  $d_0$ , and updating their beliefs about the coefficient each period using a recursive system as new observations become available. As shown in [Evans & Honkapohja \(2012\)](#), E-stability is governed by the mapping from agents' PLM to the implied ALM, defined as the T-map. In our example, the T-map is given by:

$$T : d \rightarrow T(d) = \frac{E[\pi_t r_t]}{E[r_t r_t]} = (d\rho + 1) \frac{\alpha_1(1 - p_{22}) + \alpha_2(1 - p_{11})}{\alpha_1\alpha_2(2 - p_{11}p_{22})}. \quad (2.11)$$

The T-map is locally stable if its Jacobian matrix has roots with real parts less than one. When the local stability condition is satisfied, the equilibrium is E-stable. Applying this to our RPE, the associated root and the E-stability condition are given as:

$$\frac{DT(d)}{D(d)} = \frac{\alpha_1(1 - p_{22}) + \alpha_2(1 - p_{11})}{\alpha_1\alpha_2(2 - p_{11} - p_{22})}\rho < 1, \quad (2.12)$$

which, after re-arranging, yields:

$$\alpha_1\alpha_2 > \frac{\alpha_1(1 - p_{22}) + \alpha_2(1 - p_{11})}{2 - p_{11} - p_{22}}. \quad (2.13)$$

This results in a criterion similar to that of *LRTP*. In order to obtain E-stability, a more aggressive monetary policy rule  $\alpha_1$  is needed whenever (i) the average time spent in regime 1 (given by  $P_1$ ) decreases, (ii) the average time spent in regime 2 (given by  $P_2$ ) increases, or (iii) the monetary policy rule in regime 2 ( $\alpha_2$ ) becomes less aggressive. This suggests that overall E-stability holds even if one of the underlying regimes is E-unstable, as long as there is a sufficiently E-stable regime and the system does not spend too much time in the unstable regime on average. This is an intuitive extension of [Davig & Leeper's](#) insight on long-run determinacy to the *learnability of equilibria*, therefore we denote this as *the principle of long-*

---

<sup>9</sup>See Appendix B.1 for details on the derivation of this condition.

<sup>10</sup>[Bullard & Eusepi \(2014\)](#) shows that there is a tight link between determinacy and E-stability of REE and in some special cases these conditions may even coincide.

run E-stability.

## 2.2 Regime Switches and Constant Gain Learning

The RPE concept and its associated long-run E-stability condition in (2.10) serve as a starting point to illustrate the model dynamics in our framework, and to draw parallels to previous work under REE. Building on this, our main point of interest in this paper is to study the transitory dynamics under adaptive learning when there is a monetary policy regime switch.

We first extend the model (2.10) with lagged inflation in order to also study learning dynamics about persistence. Assume that a fraction  $\iota_p$  of agents have backward-looking expectations based on the previous period, while the remaining fraction  $1 - \iota_p$  form their expectations rationally as before. This yields the following model:

$$\begin{cases} i_t = \tilde{E}_t \pi_{t+1} + r_t, \\ \tilde{E}_t \pi_{t+1} = \iota_p \pi_{t-1} + (1 - \iota_p) E_t \pi_{t+1}, \\ r_t = \rho r_{t-1} + v_t, \\ i_t = \alpha(s_t) \pi_t, \end{cases} \quad (2.14)$$

where  $\tilde{E}_t$  denotes aggregate expectations operator and  $E_t$  refers to the Rational Expectations as before. Assuming again that agents' do not observe the regime switches, the associated PLM of the rational agents is of the form:<sup>11</sup>

$$\pi_t = dr_t + b\pi_{t-1}, \quad (2.15)$$

with the associated T-map:

$$\begin{pmatrix} d \\ b \end{pmatrix} \rightarrow \begin{pmatrix} E[(\pi_t - b(s_t)\pi_{t-1})r_t] \\ \frac{E[(\pi_t - d(s_t)r_t)\pi_{t-1}]}{E[\pi_t^2]} \end{pmatrix}, \quad (2.16)$$

where  $b(s_t) = \frac{\iota_p}{\alpha(s_t) - (1 - \iota_p)b}$  and  $d(s_t) = \frac{(1 - \iota_p)d\rho + 1}{\alpha(s_t) - (1 - \iota_p)b}$ .<sup>12</sup>

Next we introduce adaptive learning into this system, where beliefs about  $d$  and  $b$  are updated each period as new observations become available, using a constant-gain least squares

---

<sup>11</sup>We assume that rational agents take into account the presence of backward-looking agents when forming their expectations.

<sup>12</sup>With the addition of lagged inflation, the moments appearing in the above expression become analytically intractable, therefore the values  $a^{RPE}$  and  $b^{RPE}$  and the associated E-stability conditions are obtained numerically in the examples below. The derivations of the RPE and regime-specific equilibria can be found in Appendix B.3 for a general N dimensional system with m regimes. The example illustrated here is a special case of 1 dimension with 2 regimes.

method à la [Evans & Honkapohja \(2012\)](#). Denoting by  $\theta = [d, b]'$  and  $y_t = [r_t, \pi_{t-1}]'$ , the agents update their regression model (i.e. the coefficients in their PLM) using:

$$\begin{cases} R_t = R_{t-1} + \gamma(y_t^2 - R_{t-1}), \\ \theta_t = \theta_{t-1} + \gamma R_t^{-1} y_t (\pi_t - \theta_{t-1} y_t), \end{cases} \quad (2.17)$$

where  $\gamma$  denotes the gain value, i.e. the weight that agents put into the most recent observation. A constant gain implies geometric discounting of the past and allows agents to put more weight into recent observations, thereby allowing them to potentially detect the consequences of regime switches. We first illustrate the model dynamics for a parameterization where both regime-specific MSV-solutions, as well as the underlying RPE are E-stable. Figure 1 shows two simulations with different gain values and transition probabilities. Panel (a) is an example with frequent regime switches,  $p_{11} = p_{22} = 0.9$ , and a small gain value of 0.005. In this case the learning coefficients oscillate around the RPE-consistent values, illustrating the stability of the system. An interesting feature of the RPE is that, while  $d^{RPE}$  is between the regime-specific equilibrium values,  $b^{RPE}$  is larger than both regime-specific values. This suggests that RPE is not always a simple weighted average of the underlying regime-specific equilibria, and that regime-switching may induce persistence amplification in the system.

Panel (b) shows an example with more persistent regimes,  $p_{11} = p_{22} = 0.99$ , and a larger gain value of 0.01. It is readily seen that when the gain value is sufficiently large and the regime durations are long, the system converges to the regime-specific values, i.e. agents forget about the past regime switches. When the regime shift occurs, there are two possible outcomes for the learning dynamics: if the RPE and the new regime specific value are in the same direction, as in the case for  $d_t$ , then the learning process gradually moves towards the direction of the new regime. If the RPE and the new regime specific value are in different directions, such as for  $b_t$  in this example, then the learning process first jumps in the direction of the RPE, before starting to gradually move towards the regime specific value. This figure illustrates that, under the right circumstances with large enough gains and frequent regime shifts, transitioning from one regime to another may be characterized by a period of temporarily amplified persistence. Importantly, this suggests that learning of the new regime can be very quick, especially when exiting a very long regime or entering into a new regime that has not been observed before. These results are in line with [Hollmayr & Matthes \(2015\)](#), where unanticipated structural change leads to a temporary period of fast learning and amplified volatility. In our framework, this phenomenon occurs as a temporary shift towards the RPE.

The characteristics discussed above are particularly important from an empirical viewpoint: the recent ELB episode is similar to such a switch from a persistent regime to a new regime that was not experienced in the recent past. This is discussed in further detail in Section 4 in

the context of the Smets & Wouters (2007) model.

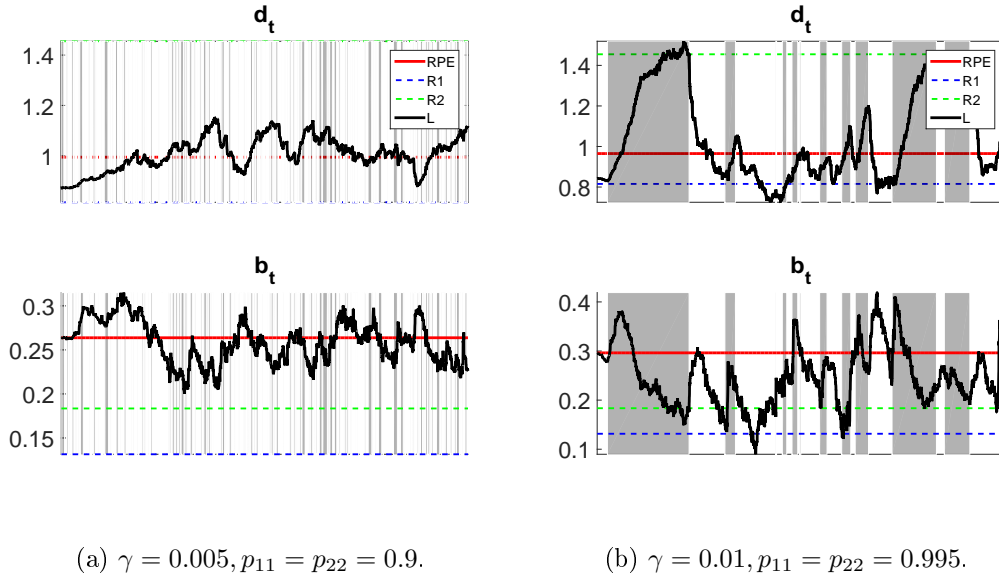


Figure 1: Learning coefficients along with the RPE-consistent and regime-specific values. The parameters  $\iota_p = 0.25, \rho = 0.9, \alpha_1 = 1.5, \alpha_2 = 2$ , are fixed in both simulations. Given the values of  $\alpha_1$  and  $\alpha_2$ , both regime-specific equilibria and the RPE are E-stable.

### 2.3 Mean Dynamics

We next consider an extension with the mean dynamics. In the previous two examples, expectations about the mean are implicitly fixed at the equilibrium value of zero and as such, expectations are *anchored* at the equilibrium. Learning about the mean dynamics introduces a possibility of de-anchoring from the equilibrium, and can therefore be interpreted as an example of imperfect anchoring as in Busetti et al. (2014).

To motivate the learning dynamics about the mean, we assume that nominal interest rates react to deviations of inflation from its non-zero target rate  $\bar{\pi}$ , i.e.  $i_t - \bar{\pi} = \alpha(s_t)(\pi_t - \bar{\pi})$ . This yields the following model:

$$\begin{cases} i_t = \tilde{E}_t \pi_{t+1} + r_t, \\ \tilde{E}_t \pi_{t+1} = \iota_p \pi_{t-1} + (1 - \iota_p) E_t \pi_{t+1}, \\ r_t = \rho r_{t-1} + v_t, \\ i_t - \bar{\pi} = \alpha(s_t)(\pi_t - \bar{\pi}), \end{cases} \quad (2.18)$$

where the rational agents' PLM is given by:

$$\pi_t = a + b\pi_{t-1} + dr_t, \quad (2.19)$$

and the T-map:

$$\begin{pmatrix} a \\ b \\ d \end{pmatrix} \rightarrow \begin{pmatrix} E[(\pi_t - b(s_t)X_{t-1} - d(s_t)\epsilon_t)] \\ E\left[\frac{(\pi_t - a(s_t) - b(s_t)\pi_{t-1})r_t}{E[r_t^2]}\right] \\ \frac{E[(\pi_t - a(s_t)d(s_t)r_t)\pi_{t-1}]}{E[\pi_t^2]} \end{pmatrix}, \quad (2.20)$$

with  $a(s_t) = \frac{(\alpha(s_t)-1)\bar{\pi}+(1-\iota_p)a}{\alpha(s_t)-(1-\iota_p)b}$ ,  $b(s_t) = \frac{\iota_p}{\alpha(s_t)-(1-\iota_p)b}$  and  $d(s_t) = \frac{(1-\iota_p)d\rho+1}{\alpha(s_t)-(1-\iota_p)b}$ . Figure 2 illustrates two simulations using the same parameterization from before with  $\bar{\pi} = 2$ , where both regime-specific equilibria and the RPE are E-stable. Panel (a) again shows frequent regime switches with a small gain value, while Panel (b) shows infrequent switches with a larger gain. We observe that in this case,  $a^{RPE}$  is lower than both regime-specific values, which confirms our result from the previous section that the RPE may not always be a simple weighted average of the regimes. The lower value of  $a^{RPE}$  suggests that the perceived inflation target is lower under RPE than both regime specific values. While we observe oscillations near the RPE in the first simulation, the second one jumps to the RPE along with regime switches, followed by a gradual movement towards the regime-specific values as the regime persists.

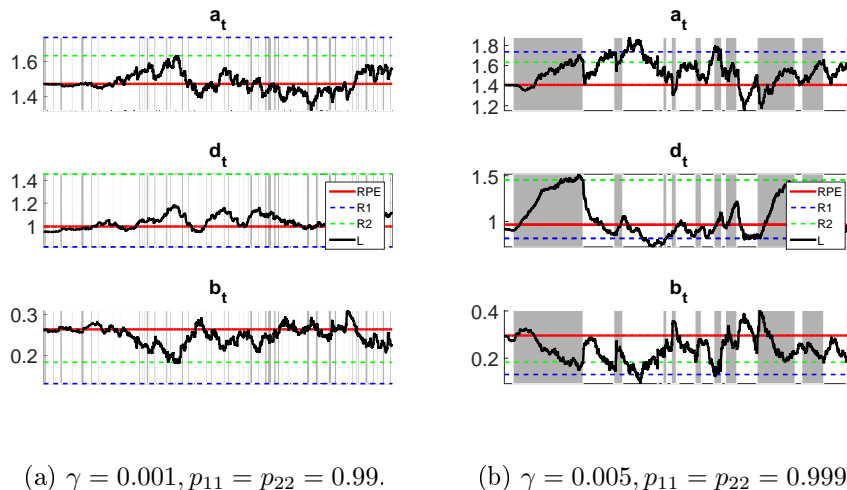


Figure 2: Learning coefficients along with the RPE-consistent and regime-specific values. The parameters  $\bar{\pi} = 2, \iota_p = 0.25, \rho = 0.9, \alpha_1 = 1.5, \alpha_2 = 2$ , are fixed in both simulations. Given the values of  $\alpha_1$  and  $\alpha_2$ , both regime-specific equilibria and the RPE are stable.

## 2.4 Effective Lower Bound and Regime-switching

Having illustrated the main concepts, in this section we establish the link between the ELB constraint and the regime-switching setup. We use a deterministic version of the baseline 3-equation New Keynesian model. Consider the standard Euler and Phillips curve equations:

$$\begin{cases} x_t = E_t x_{t+1} - \sigma(i_t - E_t \pi_{t+1}), \\ \pi_t = \beta E_t \pi_{t+1} + \kappa x_t, \end{cases} \quad (2.21)$$

with  $x_t$  output gap and  $\pi_t$  inflation, supplemented with a standard Taylor rule for monetary policy subject to the ELB constraint:  $i_t = \max\{\phi_\pi \pi_t + \phi_x x_t, -\bar{r}^*\}$ . In this section, we take  $\bar{r}^* = 0$  without loss of generality and refer to it as the zero lower bound (ZLB) constraint, while the empirical applications in the next section allow for non-zero values of  $\bar{r}^*$ . The monetary policy rule is approximated as a Markov switching process:<sup>13</sup>

$$i_t = \phi_\pi(s_t)\pi_t + \phi_x(s_t)x_t, \quad (2.22)$$

where the nominal rate  $i_t$  switches between two regimes: the first one takes the form of an active Taylor rule with  $\phi_\pi(s_t = T) > 1$  and  $\phi_x(s_t = T) > 0$ , which is the normal regime when the ZLB constraint is not binding. The second one follows a pegged interest rate rule with  $\phi_\pi(s_t = ZLB) = 0$  and  $\phi_x(s_t = ZLB) = 0$  when the ZLB constraint is binding. Similar to the previous sections, we assume transition probabilities  $p_{11}$  (for the normal regime) and  $p_{22}$  (for the ZLB regime), implying ergodic probabilities of  $P_1 = \frac{1-p_{22}}{2-p_{11}-p_{22}}$  and  $P_2 = \frac{1-p_{11}}{2-p_{11}-p_{22}}$ .

A well known result in the literature is that, when monetary policy is inactive, which corresponds to the ZLB regime in this setup, standard New Keynesian models are indeterminate and the learning dynamics are E-unstable under plausible parameterizations,<sup>14</sup> which leads to the possibility of deflationary spirals. In what follows, we establish this result in our regime-switching framework.

Denoting by  $Y_t = [x_t, \pi_t]'$ , the system can be re-written as  $Y_t = \Gamma(s_t)E_t Y_{t+1}$  with  $\Gamma(s_t) = \frac{1}{1+\sigma\phi_x(s_t)+\kappa\sigma\phi_\pi(s_t)} \begin{pmatrix} 1 & \sigma(1-\beta\phi_\pi(s_t)) \\ \kappa & \kappa\sigma + \beta(1+\sigma\phi_x(s_t)) \end{pmatrix}$ . In this simplified form, the associated law of motion (where agents ignore the presence of regime switches) takes the form of  $Y_t = a$ , that is, agents only learn about the means. The implied law of motion is then given by  $Y_t = \Gamma a$ , and the corresponding T-map is:

$$a \rightarrow T(a) = E[\Gamma(s_t)a]. \quad (2.23)$$

---

<sup>13</sup>See e.g. [Binning & Mair \(2016\)](#), [Chen \(2017\)](#) and [Lindé et al. \(2017\)](#) for earlier work, where the ELB period is analyzed in a regime-switching framework.

<sup>14</sup>see [Evans & Honkapohja \(2010\)](#) for a detailed treatment.

Recall from Section 2.1 that the long-run E-stability condition is satisfied if the real part of the largest root associated with the T-map does not exceed unity. Denoting the real part of the largest root by  $\rho(s_t)$  for each regime  $s_t$ , the long-run E-stability condition is satisfied in this case if the weighted average  $P_1\rho(s_t = T) + P_2\rho(s_t = ZLB)$  is inside the unit circle. Figure 3 illustrates the E-stability region for the RPE as a function of the ZLB exit probability  $1 - p_{22}$  for a standard parameterization. First looking at the regime-specific roots, we observe that the E-stability condition always holds for the normal regime, while the ZLB regime is E-unstable. The E-stability of the RPE depends on how much time the system spends at the ZLB regime on average (i.e. the ergodic probability), which in turn is determined by the exit probability from the ZLB regime. We observe that, for the given parameterization, exit probabilities below 5% (which translates into an average of 16.6% of all periods at the ZLB) result in an RPE that is E-unstable. Hence the system becomes E-unstable if it spends too much time at the ZLB regime on average: this corresponds to the threshold, after which deflationary spirals with ever falling output gap and inflation become dominant.<sup>15</sup>

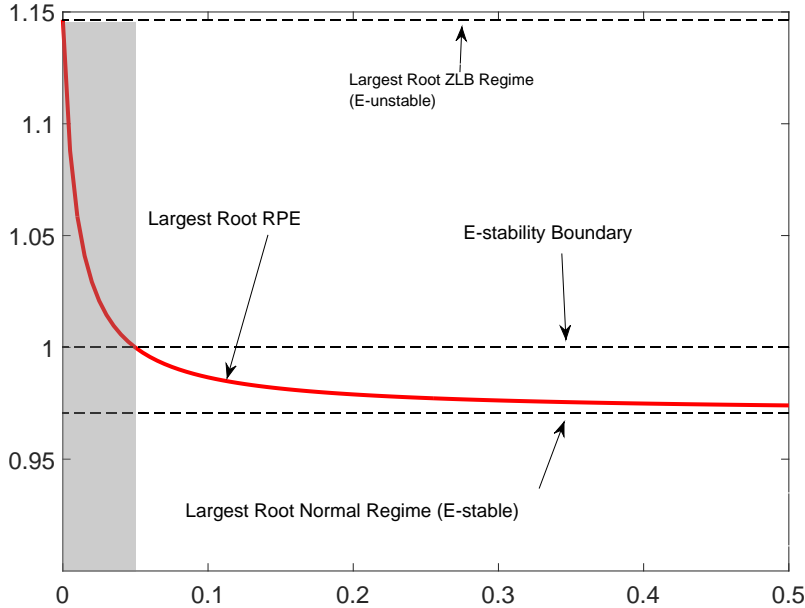


Figure 3: Largest roots for regime-specific equilibria and RPE in the New Keynesian model as a function of the ELB exit probability  $1 - p_{22}$ . We use a standard parameterization with  $\sigma = 1$ ,  $\beta = 0.99$ ,  $\kappa = 0.02$ ,  $p_{11} = 0.99$ . This parameterization closely follows Arifovic et al. (2018). The Taylor rule coefficients in the normal regime are  $\phi_\pi = 1.5$  and  $\phi_x = 0.5$ . The grey area corresponds to the region where the E-stability does not hold for the RPE.

This example is useful for illustrating the potential E-unstability of the ZLB regime. These initial results imply that spending too much time in the ZLB regime relative to the normal regime can destabilize the economy. However, the transition probabilities are exogenous in this

---

<sup>15</sup>Further details about the derivations, and a small extension with exogenous AR(1) shocks can be found in Appendix B.4.

example and as such, it does not provide an insight on how the economy exits the ZLB. Indeed, if the ZLB regime is associated with worsening macroeconomic conditions, the economy may be stuck at the ZLB regime by giving rise to deflationary spirals and a falling output, which makes it harder to leave the ZLB. We explore such cases in Sections 4 and 4.6 with endogenous switching models, where the transition matrix  $Q$  is time-varying and dependent on the nominal interest rates implied by the Taylor rule. In the next section, we first present the general multivariate setup and discuss the empirical methodology.

### 3 General Setup and Estimation

This section introduces the general class of linear multivariate models, subject to regime switches and adaptive learning. Consider the following data generating process:

$$\begin{cases} X_t = A(s_t) + B(s_t)X_{t-1} + C(s_t)E_t X_{t+1} + D(s_t)\epsilon_t, \\ \epsilon_t = \rho\epsilon_{t-1} + \eta_t, \end{cases} \quad (3.1)$$

where  $X_t$  denotes the state-variables that may depend on their lags  $X_{t-1}$ , 1-step ahead expectations  $E_t X_{t+1}$  and the structural shocks  $\epsilon_t$ . We assume the exogenous shocks follow a general VAR(1) process with matrix  $\rho$ , while the matrices  $A$ ,  $B$ ,  $C$ ,  $D$  and  $E$  contain the structural parameters of the model. A subset of the structural parameters are subject regime switches, captured by  $s_t$ .<sup>16</sup> The corresponding PLM of agents are period specific but independent of regime switches, given by:

$$\begin{cases} X_t = a_{t-1} + b_{t-1}X_{t-1} + d_{t-1}\epsilon_t, \\ E_t X_{t+1} = a_{t-1} + b_{t-1}X_t + (d_{t-1}\rho)\epsilon_t, \end{cases} \quad (3.2)$$

where we use a *period t dating* assumption for expectations, i.e. the structural shocks and contemporaneous variables are jointly determined with the 1-step ahead expectations.<sup>17</sup> The PLM parameters  $a_{t-1}$ ,  $b_{t-1}$  and  $d_{t-1}$  are updated *after* the state variables are realized, hence they enter into (3.2) with a lag. The above specification conveniently nests all PLMs that we use in our estimation exercises, which is discussed below. Plugging the expectations in (3.2) back into (3.1) yields the implied ALM:

$$X_t = A(s_t) + B(s_t)X_{t-1} + C(s_t)a_{t-1} + C(s_t)b_{t-1}X_t + (C(s_t)(d_{t-1}\rho) + D(s_t))\epsilon_t, \quad (3.3)$$

---

<sup>16</sup>Note that we abstract away from regime switches in the structural shocks here without loss of generality.

<sup>17</sup>The alternative is to use period t-1 dating, which assumes a sequential timeline where expectations are determined based on period t-1 information, after which period t shocks and contemporaneous variables are determined. The results reported in the paper are not sensitive to this assumption.

which can be re-written as:

$$X_t = a_{t-1}(s_t) + b_{t-1}(s_t)X_{t-1} + d_{t-1}(s_t)\epsilon_t, \quad (3.4)$$

with  $a(s_t) = (I - C(s_t)b_{t-1})^{-1}(A(s_t) + C(s_t)a_{t-1})$ ,  $b(s_t) = (I - C(s_t)b_{t-1})^{-1}B(s_t)$  and  $d(s_t) = (I - C(s_t)b_{t-1})^{-1}(C(s_t)(d_{t-1}\rho) + D(s_t))$ .<sup>18</sup> Denoting by  $\Phi_t = [a_t, d_t, b_t]'$  and  $Y_t = [X_{t-1}, \epsilon_t]'$ , the coefficients in agents' PLM are updated using constant gain recursive least squares:

$$\begin{cases} R_t = R_{t-1} + \gamma(Y_t Y_t' - R_{t-1}), \\ \Phi_t = \Phi_{t-1} + \gamma R_t^{-1} Y_t (X_t - \Phi_{t-1} Y_t)' . \end{cases} \quad (3.5)$$

The system is characterized by two types of time variation, which can be written in the following compact state-space form:

$$S_t = \gamma_{0,\Phi_{t-1}}^{(s_t)} + \gamma_{1,\Phi_{t-1}}^{(s_t)} S_{t-1} + \gamma_{2,\Phi_{t-1}}^{(s_t)} \eta_t, \quad , \eta_t \sim N(0, \Sigma), \quad (3.6)$$

with  $S_t = [X_t', \epsilon_t']'$  and  $\gamma_{0,\Phi_t}^{(s_t)}$ ,  $\gamma_{1,\Phi_t}^{(s_t)}$  and  $\gamma_{2,\Phi_t}^{(s_t)}$  conformable matrices in terms of structural parameters, which depend on the assumption of the PLM. We next discuss the estimation of this general model in (3.6).

### 3.1 Estimation

The standard filtering algorithm for Markov-switching state-space models is the modified Kalman filter by [Kim & Nelson](#) ( henceforth KN-filter): in a Markov-switching model with  $m$  regimes, a dataset of size  $T$  leads to  $m^T$  possible timelines, which quickly makes the standard Kalman filter intractable as  $T$  grows. The main idea in the KN-filter is to introduce a so-called *collapsing* technique to deal with this issue, which amounts to taking weighted averages of the state vector and covariance matrix at each iteration of the filter. This effectively reduces the number of timelines at each iteration by an order of  $m$ , thereby making the filter tractable for large values of  $m$  and  $T$ . The standard recommendation for collapsing is to carry as many lags of the states as there are in the transition equations, therefore we consider a version of the filter with a single lag. Accordingly, if there are  $m$  different regimes in the model, we carry  $m$  different timelines in each period. This introduces  $m^2$  different sets of variables in the forecasting and updating steps, which are collapsed at the end of each iteration to reduce the system to  $m$  sets of variables.

An important question is how to introduce adaptive learning into this framework. We use

---

<sup>18</sup> Appendix B.3 provides the first and second moments that appear here for a general setup with  $m$  regimes. In this general framework, the values associated with the equilibrium intractable. Therefore the E-stability of a given model can only be assessed via Monte Carlo simulations.

an approach that is consistent with the theoretical framework of the previous section: the agents have a unique PLM based on observables, independent of the regime switches. We model this formally by collapsing the  $m$  different states further at each iteration to obtain the final states estimated by the filter, which are used for the adaptive learning step. The unique learning coefficients are then used in each Kalman filter timeline of the next period's iteration.<sup>19</sup> Adding a set of measurement equations to (3.6) yields the state-space representations:

$$\begin{cases} S_t = \gamma_{0,\Phi_t}^{(s_t)} + \gamma_{1,\Phi_t}^{(s_t)} S_{t-1} + \gamma_{2,\Phi_t}^{(s_t)} \eta_t, & , \eta_t \sim N(0, \Sigma) \\ y_t = E + F S_t, \end{cases} \quad (3.7)$$

for a set of observable variables  $y_t$ . Figure 4 illustrates the KM-filter for the special case of two regimes.<sup>20</sup> The filter yields the likelihood function as a side-product, which is combined with a set of prior distributions for Bayesian inference. Importantly, the filter is flexible enough to accommodate both exogenous and endogenous regime transition probabilities, and we discuss both versions in Section 4.

### 3.2 Initial Beliefs

A first practical issue in empirical studies on learning is how to initialize the beliefs. Initial beliefs have been shown to play a key role in driving the estimation results and model fit in previous studies, and various different approaches have been considered: [Milani \(2007\)](#) uses an estimation-based approach, where the initial beliefs are treated as free parameters and estimated jointly along with the other structural parameters of the model; [Slobodyan & Wouters \(2012a, 2012b\)](#) consider REE-based and training-sample based approaches along with the estimation-based approach; while [Berardi & Galimberti \(2017c\)](#) proposes a smoothing-based approach. A common result in these studies is that the results are generally sensitive to initial beliefs, and the best-fitting approach depends on the specific model under consideration; see [Berardi & Galimberti \(2017a, 2017b\)](#) for a detailed overview on initial beliefs.

Our goal in this paper is to take a minimal deviation from the REE framework and therefore we follow the approach in [Slobodyan & Wouters \(2012b\)](#) with REE-based initial beliefs. Accordingly, for each parameter draw, the REE of the model is computed as a first step.<sup>21</sup> Then the relevant moments from this equilibrium are used as initial beliefs for the learning models.

---

<sup>19</sup>A natural alternative here is to apply the adaptive learning step distinctly to each collapsed state; one can then take a weighted average of these expectations to obtain the filtered expectations. Our results in the upcoming sections are not sensitive to such an alternative, but we only present the results under the first approach since it is more in the spirit of our theoretical framework.

<sup>20</sup>see Appendix C for details on the filter.

<sup>21</sup>Since the initial 40 years of our sample is governed by an active Taylor rule, we use the REE solution consistent with the normal regime.

$$\begin{cases} S_t = \gamma_{0,\Phi_t}^{(s_t)} + \gamma_{1,\Phi_t}^{(s_t)} S_{t-1} + \gamma_{2,\Phi_t}^{(s_t)} \eta_t, & , \eta_t \sim N(0, \Sigma) \\ y_t = E + F S_t. \end{cases}$$

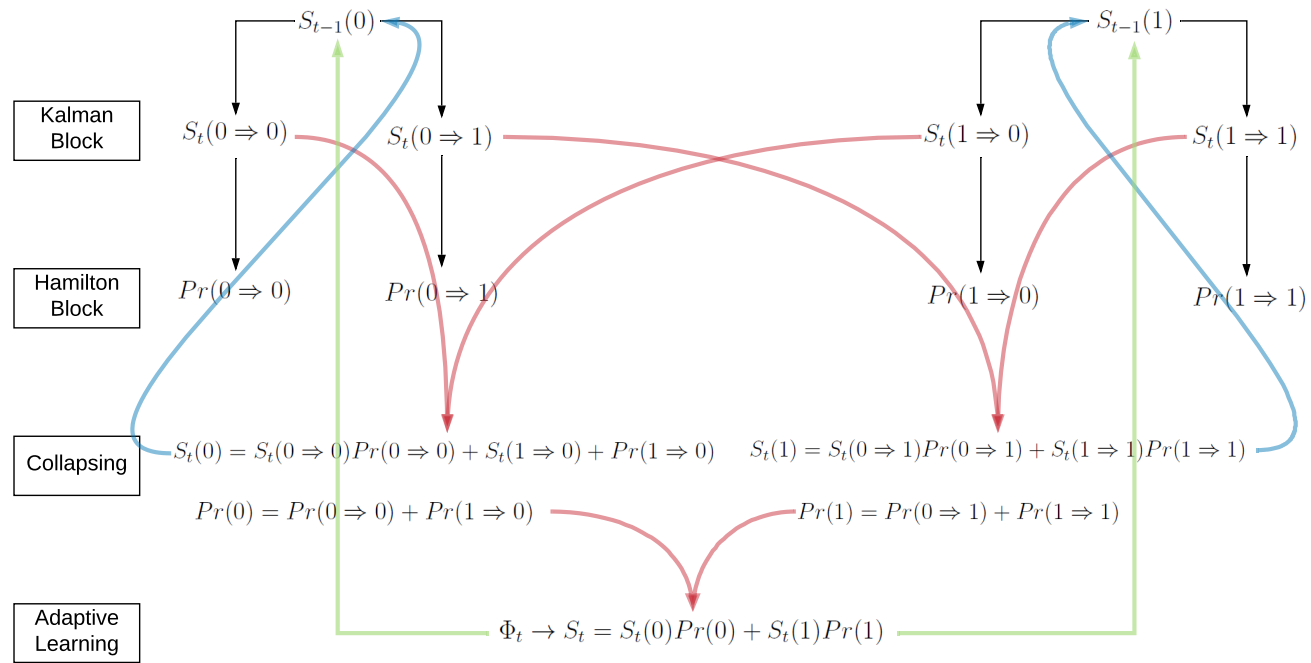


Figure 4: Illustration of the filter in a 2-regime model.

### 3.3 Projection Facilities

A second issue with the estimation of adaptive learning models relates to projection facilities. A well-known issue with constant gain recursive least squares is that the stationarity of the underlying models is not always guaranteed. Particularly when the PLM involves lagged state variables, the learning process may occasionally push the system into non-stationary and explosive regions, even if the underlying equilibrium is E-stable.<sup>22</sup>

A common method in the adaptive learning literature to deal with these potential instabilities is to impose a projection facility on the model, which forces the model dynamics to be stationary by projecting the learning coefficients into the stable region whenever instability is encountered. The simplest approach is to leave the learning coefficients at their previous value if the update leads to non-stationarity, which is the method adopted in [Slobodyan & Wouters \(2012a\)](#). Specifically in our estimations, we set up the projection facility as follows: if the learning update pushes the largest root of the ergodic distribution associated with the model (3.6) outside the unit circle in a period, then we stop updating the learning coefficients for that period. In other words, we allow the regime-specific dynamics to be temporarily non-stationary as long as the underlying implied ergodic distribution remains stable. Importantly, this approach allows the agents' PLM (3.2) to become temporarily explosive as long as the underlying ergodic distribution is stable. This approach reflects our inclination to keep the projection facility as inactive as possible.

### 3.4 Learning Rules

Our discussion about learning up to this point has been based on the information set consistent with the MSV-REE solution, where the only source of misspecification is due to unobserved regimes. However, in principle, any information set may be considered in the agents' PLM. In our estimation exercises, we will focus on three types of learning rules that have been frequently used in the literature:

- (i) An MSV-consistent rule as discussed before. For this rule, the limiting case with no learning ( $\gamma = 0$ ) corresponds to an equilibrium consistent with a REE of the normal regime, where agents do not pay any attention to the potential ELB episodes.
- (ii) A VAR-like rule, which assumes unobserved shocks but otherwise keeps the same set of state variables as in the MSV solution.<sup>23</sup> [Chung & Xiao \(2013\)](#) analyze a similar setup

---

<sup>22</sup>We do not explore the formal link between indeterminacy, E-unstability and the instability due to updating. However, since an inactive monetary policy implies indeterminacy and E-unstability for the regime-specific dynamics, occasional escapes to non-stationary regions are more frequent when the ELB constraint is binding.

<sup>23</sup>In terms of (3.2), this assumes  $d$  is a zero matrix, but keeps the same  $b$  matrix as in the MSV solution.

and define it as a Limited Information Equilibrium. Therefore we refer to this learning rule as *Limited Information Learning* (LIL).

(iii) A parsimonious AR(1) rule, which ignores cross-correlations and assumes a univariate process for each forward-looking variable.<sup>24</sup> This type of univariate forecasting rules have been applied in recent past to improve the empirical fit of otherwise standard DSGE models, see e.g. [Slobodyan & Wouters \(2012b\)](#), [Gaus & Gibbs \(2018\)](#), [Di Pace et al. \(2016\)](#) and [Hommes et al. \(2019\)](#).<sup>25</sup>

## 4 Estimation of the Smets-Wouters Model

### 4.1 Priors and Measurement Equations

In this section we estimate a version of the Smets-Wouters (2007) model under adaptive learning, subject to the ELB. The details of the model are omitted here for brevity, see Appendix E for a detailed explanation of the log-linearized model equations. We have two minor deviations from the benchmark model: first, we assume the price and wage mark-up shocks follow exogenous AR(1) processes, instead of the original ARMA(1,1) assumption.<sup>26</sup> Second, we shut off the flexible economy side of the model, which is used in the original model to obtain the potential output and the associated level of output gap. Instead, we follow [Slobodyan & Wouters \(2012a\)](#) and derive the output gap from the natural level of output, based on the underlying productivity process. This has the advantage of reducing the size of the model, thereby making its estimation computationally less demanding. The rest of the model, along with the prior distributions and measurement equations remain unchanged. The monetary policy rule follows the same 2-regime structure as in Section 2.4 with some additional parameters, given by:

$$\begin{cases} i_t(s_t = T) = \rho i_{t-1} + (1 - \rho)(\phi_\pi \pi_t + \phi_x x_t) + \phi_{\Delta x}(x_t - x_{t-1}) + \varepsilon_{r,t}^T, \\ i_t(s_t = ELB) = \varepsilon_{r,t}^{ELB}, \end{cases} \quad (4.1)$$

where  $\phi_\pi$  and  $\phi_x$  are inflation and output gap reaction parameters as before, while  $\phi_{\Delta x}$  and  $\rho$  are output gap growth reaction and interest rate smoothing respectively.  $\varepsilon_{r,t}^T$  denotes an AR(1) monetary policy shock during the normal regime with persistence  $\rho_r$  and standard deviation  $\eta_r^T$ , while  $\varepsilon_{r,t}^{ELB}$  is an i.i.d. policy shock process during the ELB regime with standard deviation

---

<sup>24</sup>In terms of (3.2), this assumes  $d$  is a zero matrix and  $b$  is diagonal.

<sup>25</sup>A number of experimental studies also provide support in favor of small, parsimonious forecasting rules. See e.g. [Anufriev et al. \(2019\)](#).

<sup>26</sup>This is due to the fact that, as shown in [Slobodyan & Wouters \(2012a\)](#), these shock processes are typically close to being white noise when expectations are based on small learning rules, in which case the AR(1) and MA(1) terms are close to being locally unidentified. Therefore we assume away the MA(1) terms in these shocks.

$\eta_r^{ELB}$ .<sup>27</sup> The estimation is based on seven observables on the U.S. data over the period 1966:I-2016:IV as follows:

$$\begin{cases} d(\log(y_t^{obs})) = \bar{\gamma} + (y_t - y_{t-1}), \\ d(\log(c_t^{obs})) = \bar{\gamma} + (c_t - c_{t-1}), \\ d(\log(inv_t^{obs})) = \bar{\gamma} + (inv_t - inv_{t-1}), \\ d(\log(w_t^{obs})) = \bar{\gamma} + (w_t - w_{t-1}), \\ \log(l_t^{obs}) = \bar{l} + l_t, \\ (\log(\pi_t^{obs})) = \bar{\pi} + \pi_t, \\ (\log(i_t^{obs})) = \bar{i}(s_t) + i_t, \end{cases}$$

where  $d(\log(y_t^{obs}))$ ,  $d(\log(c_t^{obs}))$ ,  $d(\log(inv_t^{obs}))$  and  $d(\log(w_t^{obs}))$  denote real output, consumption, investment and wage growths with the common growth rate  $\bar{\gamma}$  respectively, while  $\log(l_t^{obs})$ ,  $(\log(\pi_t^{obs}))$  and  $(\log(i_t^{obs}))$  denote (normalized) hours worked, inflation rate and federal funds rate respectively. We assume a regime switch in the steady-state level of nominal interest rates, denoted by  $\bar{i}(s_t = T) = \bar{i}^T$  and  $\bar{i}(s_t = ELB) = \bar{i}^{ELB}$  respectively. We use quarterly data over the period 1966:I to 2016:IV in our estimations.

We first discuss the estimation results for the exogenous switching models, for which there are five additional parameters due to regime switching and learning that are not present in the benchmark REE model. In terms of the regime transition probabilities, we estimate the exit probabilities from the normal and ELB regimes, denoted as  $1 - p_{11}$  and  $1 - p_{22}$  respectively. We use uniform priors over  $[0, 1]$  to assess how informative the data is about these two parameters. This differs from previous studies in the literature where typically more informative priors have been used, see e.g. [Ji & Xiao \(2016\)](#), [Chen \(2017\)](#) and [Lindé et al. \(2017\)](#), all of which use tight Beta priors for the transition probabilities. For the constant gain parameter, we use a Gamma prior with mean 0.035 and standard deviation 0.03, which follows from [Slobodyan & Wouters \(2012b\)](#). This distribution permits a prior credible interval over the range  $[0, 0.1]$  for the gain, which is consistent with previous findings in the learning literature. For the standard deviation of monetary policy shocks of the ELB regime  $\eta_r^{ELB}$ , we use a Gamma distribution with mean 0.03 and standard deviation 0.01. And finally for the steady-state level of interest rates at the ELB regime, we use a normal distribution with mean 0.05 and standard deviation 0.025.

The model features seven forward looking variables, namely the rental rate of capital  $rk_t$ , asset price  $q_t$ , consumption  $c_t$ , investment  $I_t$ , labor  $l_t$ , inflation  $\pi_t$  and real wages  $w_t$ ; along with seven AR(1) structural shocks, namely technology  $\varepsilon_{a,t}$ , government spending  $\varepsilon_{g,t}$ , risk premium  $\varepsilon_{b,t}$ , investment-specific technology  $\varepsilon_{I,t}$ , monetary policy  $\varepsilon_{r,t}^T$  and  $\varepsilon_{r,t}^{ELB}$  in normal and ELB

---

<sup>27</sup>The presence of monetary policy shocks at the ELB is motivated by the fact that the nominal rates in the U.S. were not constant during 2009-2016 but was rather characterized by small changes.

regimes, and two mark-up shocks in prices  $\varepsilon_{p,t}$  and wages  $\varepsilon_{w,t}$  respectively. Further, there are seven state variables that appear with a lag in the model, namely, consumption  $c_t$ , investment  $I_t$ , output  $y_t$ , inflation  $\pi_t$ , real wage  $w_t$ , nominal interest rate  $i_t$  and capital  $k_t$ . This translates into a learning matrix of size 7x15 for the MSV model (intercept, lagged state variables and shocks), 7x8 for the LIL model (intercept and lagged state variables) and 2x1 for each variable in the AR(1) model (intercept and own lagged variable).

## 4.2 Posterior Results: Exogenous Switching Models

Using the KM-filter as illustrated in Figure 4, we first obtain the posterior mode of the likelihood using standard optimization algorithms. The estimated mode is used to initialize the MCMC to sample from the posterior distribution, for which we use a standard Random Walk Metropolis Hastings with an adaptive covariance matrix for the proposal density. We simulate two chains of length 250000 for each model under consideration, and the first 40% of the chains is discarded as the transient period. The remaining 150000 draws are checked for convergence using standard tests of [Geweke \(1992\)](#) within the chain, [Gelman et al. \(1992\)](#) between the chains.

Tables 2 and 3 show the results for the three learning models, as well as the MS-REE model and REE benchmark case. First comparing the (log-) marginal densities of the models, we observe that the Markov-Switching REE model (REE-MS) yields a substantial improvement over the benchmark REE: based on the Modified Harmonic Mean (MHM) estimators of -1194 and -1145, we obtain a Bayes Factor of 21.54 in favor of the Markov-switching model. Next comparing the learning models with REE-MS,<sup>28</sup> we observe that all three learning models yield an improvement over REE-MS, but to varying degrees: MSV-learning results in a small (and negligible) improvement, while the LIL and AR(1) models result in relatively large improvements. The corresponding Bayes Factors relative to the REE benchmark are 21.97, 35.87 and 31.09 for MSV, LIL and AR(1) respectively, which translate into Bayes Factors of 0.43, 14.32 and 9.55 relative to the REE-MS model. This indicates that, while the time-variation due to expectations under MSV-learning does not generate a meaningful improvement in the model fit, the LIL and AR(1) models yield a further improvement over REE-MS. Among the three learning models, LIL specification emerges as the preferred model based on the marginal densities.

The estimated parameters generally remain similar across REE and REE-MS models. The differences between these models and the MSV-learning also remain modest. But when we compare the REE and REE-MS models to the remaining two learning models of LIL and AR(1), some notable differences emerge.

---

<sup>28</sup>It is readily seen from Tables 2 and 3 that, while the Laplace and MHM estimators of marginal likelihood result in similar values for REE and REE-MS models, there is some discrepancy between these two estimators for the learning models. Therefore our discussion is based on the MHM estimator throughout the remainder of the paper.

We start by discussing the estimated regime transition probabilities and gain parameters. The exit probability from the normal regime,  $1 - p_{11}$ , is similar across all four regime-switching models. The posterior mean for this parameter oscillates between 0.99% and 1.14%, which translates into an expected duration between 101 and 88 quarters. The HPD intervals for this regime are overlapping across all models. However, the exit probability from the ELB regime,  $1 - p_{22}$ , turns out quite different between REE-MS and the learning models. The REE model attaches a high probability to leaving the ELB regime: at the posterior mean, the exit probability is nearly 30%, implying a short expected duration of only 3.3 quarters. For the learning models, this number decreases to values between 3.8% and 6.6%, with implied expected durations between 15 and 26 quarters, closer to the empirical duration of the ELB for the U.S. economy. It is also important to note that the implied HPD bands under REE and all three learning models for this parameter are mutually exclusive: the highest upper bound of the 90% HPD interval across the learning models is 15.3% LIL model, whereas the lower bound for REE-MS model is at 23%. This shows that the REE-MS model favors a low expected ELB duration due to agents' expectations. But since the model equates subjective and objective expectations about leaving the ELB regime, this creates a trade-off between generating a short expected duration on the agents' part, and matching the empirical duration of the ELB episode. Over the duration of the ELB period, this result suggests that the agents are constantly surprised as the regime persists, since they expect to stay at the ELB for only 3.3 quarters. The learning models, by breaking the tight link between subjective and objective expectations, allow the model to generate a more persistent and realistic ELB duration.

The resulting filtered (one-sided) average regime probabilities for some of the key periods are reported for all regime-switching models in Table 1.<sup>29</sup> We observe some differences in the estimated probabilities across models both during the entry and exit: in 2008Q3, the AR(1)-learning and REE-MS models attach a 0% probability to the ELB regime, while this number is 34.6% for the LIL model, and 96.6% for the MSV-learning model. The probabilities increase to 67.1% and 91.8% in 2008Q4 for the AR(1) and REE-MS models, while they are at 98.5% and 99.9% for the LIL and MSV models. From 2009Q1 onwards, all models attach a probability near 100% to the ELB regime until the end of 2015Q1.

Compared to the estimated entry probabilities, we observe larger differences around the ELB exit dates. The AR(1) and REE-MS models imply that the economy exits the ELB regime from 2015Q2 onwards, with probabilities near 0% until the end of our sample period. In this case the LIL model yields similar results to these two models, with ELB regime probabilities oscillating around 10% after 2015Q1. Compared to the other three, the MSV model yields a different result, where the ELB regime probability stays close to 100% until the end of our

---

<sup>29</sup>The probabilities are obtained by averaging 10000 runs of the filter, where the parameter draws are taken from the last 20% of the MCMC simulations with a thinning factor of 0.2.

sample period. The observed differences in both the entry and exit result from the interest rates implied by the Taylor rule during the normal regime. Recall that monetary policy reacts to inflation and output gap during the normal regime. While inflation is an observed variable (and thus it is common across the models), the output gap process is unobserved and estimated differently in each model. As such, the differences in the estimated Taylor rule parameters, as well as the differences in the filtered output gap processes contribute to the differences between the estimated regime probabilities.

Among the learning models, the estimated gain parameter is smallest for the MSV-learning model with a mean of 0.0012, and highest for the LIL model with a mean of 0.0064. Compared to the LIL model, the AR(1) model yields a slightly lower gain with a mean of 0.005. These values suggest that the MSV-learning model with the largest information set results in the slowest update of learning coefficients, while the remaining two models generate comparable levels of updating speed. The implications for the time-variation in the learning coefficients will be discussed further in the next subsection.

Next we turn to shock and persistence parameters that mainly affect the autocorrelation and cross-correlation dynamics in the model. Some parameters that have similar effects on model dynamics are discussed in groups. The first of these groups is habit persistence  $\lambda$  and risk premium shock persistence  $\rho_b$ , both of which generate persistence in consumption Euler and the asset pricing equations. We observe that, on the one hand for REE and MSV-learning models, habit persistence is lower with values of 0.75 and 0.76, compared to the other three models with values between 0.78 and 0.85. On the other hand, for the low habit models, the shock persistence is somewhat higher with values of 0.45 and 0.42, compared with the other high habit models where the persistence varies between 0.25 and 0.34. Overall, all parameters are within the HPD bands of each other, suggesting similar consumption and asset pricing dynamics across all models.

Next considering wage dynamics, we discuss the wage stickiness  $\xi_w$ , wage indexation  $\iota_w$  and wage mark-up shock persistence  $\rho_w$ : these parameters mainly affect the wage setting dynamics, and it is readily seen that all three parameters are estimated at similar values across REE, REE-MS and MSV-learning models. In particular, we observe high degrees of stickiness varying between 0.93 and 0.94, as well as high degrees of indexation varying between 0.79 and 0.82. This is combined with low shock persistence values in the interval [0.07, 0.12]. For the LIL and AR(1) models, we observe similarly low levels of shock persistence with values of 0.14 and 0.1 respectively, but in these models we also obtain a lower wage stickiness with 0.82 and 0.76, combined with a lower wage indexation with 0.67 and 0.55 respectively. This suggests that the change in the information set from MSV-learning to LIL and AR(1)-learning results in more persistence, which in turn yields smaller estimates for these friction parameters.

Looking at the Phillips curve and inflation dynamics with a focus on price stickiness  $\xi_p$ , price

indexation  $\iota_p$  and price mark-up shock persistence  $\rho_p$ , we observe a similar story compared to the wage dynamics. The parameter estimates are similar across REE, REE-MS and MSV-learning models with a price stickiness between 0.79 and 0.83, a price indexation between 0.1 and 0.11 and a shock persistence between 0.7 and 0.78. This suggests that the roles of shock persistence and indexation change for these models compared to the wage setting dynamics. For the LIL and AR(1) models, the price stickiness comes out similar to the other models with 0.79 and 0.74, while the price indexation is somewhat higher with 0.27 and 0.29. However, this slightly larger indexation is offset by a substantially lower shock persistence with 0.08 and 0.05 respectively. Taken together, these parameters suggest that LIL and AR(1) models generate more persistence internally through expectations, which reduces the reliance on the exogenous persistence parameters.

Among the remaining shocks, we observe a similar difference in the estimated investment shock persistence  $\rho_i$ , which is lower under LIL and AR(1) models with 0.59 and 0.52, while this number increases to values between 0.76 and 0.81 in the remaining models. Similar to the inflation and wage dynamics, this suggests more internal persistence for the investment dynamics under LIL and AR(1) models. Due to the differences in estimated persistence parameters, the standard deviations for risk premium and investment shocks,  $\eta_b$  and  $\eta_i$ , turn out higher under LIL and AR(1) models compared to the others. These larger standard deviations make up for the lower persistence parameters in the two models, resulting in similar levels of volatility for the corresponding AR(1) shock processes. Finally, the government spending and productivity shocks are both similar across all models specifications in terms of persistence and standard deviations: the productivity shock persistence  $\rho_a$  varies between 0.94 and 0.98, while the government spending shock persistence varies between 0.98 and 0.99. Similarly, the impact of productivity on government spending, captured by  $\rho_{ga}$ , varies between 0.5 and 0.53 across all models.

In terms of the measurement equation parameters, we find that the estimated steady-state of inflation  $\bar{\pi}$  is somewhat lower under LIL and AR(1) models with 0.63 and 0.67 respectively, while it is between 0.73 and 0.76 among the remaining models. This is due to the perceived mean dynamics: for these two models, the perceived mean remains substantially above zero over the estimation period, compared to the MSV-learning model where the perceived mean varies very little prior to the crisis, and the no-learning models where the perceived mean remains fixed at zero. For the remaining two parameters, the common growth rate  $\bar{\gamma}$  turns out similar across all models with values between 0.38 and 0.41, while the steady-state labor  $\bar{l}$  yields large difference across all models accompanied by wide HPD intervals, suggesting a large uncertainty around the estimates for this parameter.

We do not observe notable differences in the remaining parameters. In particular, the monetary policy parameters are similar across all models, with HPD intervals well within the

range of each other. Inflation reaction  $\phi_\pi$  ranges between 1.35 and 1.72 across all models, while these number are [0.85, 0.89] for interest rate smoothing  $\rho$ , [0.06, 0.12] for output gap reaction  $r_y$ , and [0.14, 0.19] for output gap growth reaction  $r_{dy}$ . Similarly, for Frisch elasticity of labor supply  $\frac{1}{\sigma_l}$ , we find values between 0.38 and 0.55, while for elasticity of intertemporal substitution  $\frac{1}{\sigma_c}$ , these values turn out to be 0.77 and 0.93. The posterior mean for capital adjustment cost  $\phi$  takes on values between 4.84 and 6.47 (with relatively large HPD bands, so that none of the estimated HPD bands are mutually exclusive), while the share of fixed cost in production  $\phi_p$  oscillates between 1.53 and 1.64. Similarly, the capital utilization adjustment cost  $\psi$  remains at comparable levels across all models with values between 0.64 and 0.77, and the share of capital in production  $\alpha$  ranges between 0.17 and 0.19. The household discount factor  $\beta$ , defined as  $\beta = \frac{1}{1 + \frac{\beta}{100}}$  ranges between 0.997 and 0.998, given the estimated values of  $\bar{\beta}$ .

The persistence of investment shock also becomes substantially smaller.

Date	Model			
	AR(1)	LIL	MSV	REE-MS
08Q2	0%	0%	0%	0%
08Q3	0%	34.6%	96.6%	0%
08Q4	67.1%	98.5%	99.9%	91.8%
09Q1	95.6%	98.9%	99.9%	99.3%
15Q1	99.6%	99.6%	99.9%	98.1%
15Q2	0.6%	9.4%	99.4%	0%
15Q3	1.2%	13.2%	98.4%	0%

Table 1: Estimated ELB regime probabilities during some of the important periods.

Para	Prior Dist	Mean	REE		REE-MS		MSV		LIL		AR(1)	
			Mean	HPD 90%								
$\phi$	Normal	4	5.37	3.54	7.14	6.47	4.67	8.41	5.43	3.71	7.17	4.84
$\sigma_c$	Normal	1.5	1.3	1.11	1.51	1.16	1.34	1.16	0.98	1.39	1.07	0.99
$\lambda$	Beta	0.7	0.75	0.66	0.83	0.82	0.76	0.88	0.76	0.85	0.85	0.78
$\xi_w$	Beta	0.5	0.93	0.91	0.95	0.94	0.92	0.95	0.93	0.9	0.95	0.82
$\sigma_l$	Normal	2	2.11	0.95	3.12	1.83	0.51	3.19	2.12	0.74	3.39	2.65
$\xi_p$	Beta	0.5	0.81	0.76	0.86	0.83	0.78	0.87	0.79	0.74	0.85	0.79
$t_{lw}$	Beta	0.5	0.81	0.7	0.93	0.79	0.65	0.93	0.82	0.69	0.94	0.67
$t_p$	Beta	0.5	0.10	0.03	0.17	0.11	0.03	0.21	0.11	0.03	0.21	0.27
$\psi$	Beta	0.5	0.77	0.65	0.9	0.75	0.59	0.9	0.64	0.46	0.83	0.67
$\phi_p$	Normal	1.25	1.53	1.41	1.66	1.64	1.48	1.79	1.54	1.41	1.67	1.43
$r^{\pi}$	Normal	1.25	1.49	1.24	1.75	1.47	1.17	1.82	1.72	1.41	2.04	1.35
$\rho$	Beta	0.75	0.85	0.82	0.89	0.87	0.83	0.91	0.86	0.82	0.89	0.87
$r^y$	Normal	0.125	0.06	0.03	0.10	0.07	0.03	0.12	0.12	0.06	0.18	0.11
$r^{\Delta y}$	Normal	0.125	0.18	0.14	0.21	0.18	0.14	0.21	0.19	0.15	0.23	0.17
$\bar{\pi}$	Gamma	0.625	0.74	0.58	0.89	0.76	0.57	0.98	0.73	0.58	0.93	0.63
$\bar{\beta}$	Gamma	0.25	0.15	0.06	0.24	0.15	0.05	0.26	0.2	0.08	0.33	0.18
$\bar{l}$	Normal	0	-0.11	-1.71	1.55	0.42	-1.58	2.41	1.44	0.1	2.91	0.32
$\bar{\gamma}$	Normal	0.4	0.38	0.36	0.41	0.41	0.38	0.43	0.41	0.39	0.44	0.41
$\alpha$	Normal	0.3	0.19	0.17	0.22	0.19	0.16	0.22	0.17	0.14	0.21	0.19
Mode			-1112.17		-1043.09		-1041.5		-1010.1		-1024.9	
Laplace			-1194.87		1145.02		-1136.75		-1115.38		-1126.85	
MHM			-1194.72	1	-1145.12		-1144.11	21.97	-1112.19		-1123.18	
(log-) Bayes F.								35.87			31.09	

Table 2: Estimation period: 1966:I-2016:IV, exogenous switching models.

Para	Prior Dist	REE		REE-MS		MSV		LIL		AR(1)	
		Mean	HPD 90%	Mean	HPD 90%						
$\rho_a$	Beta	0.5	0.96	0.95	0.98	0.98	0.98	0.91	0.97	0.96	0.99
$\rho_b$	Beta	0.5	0.45	0.22	0.69	0.34	0.18	0.51	0.42	0.24	0.25
$\rho_g$	Beta	0.5	0.98	0.98	0.97	0.99	0.98	0.97	0.98	0.96	0.98
$\rho_i$	Beta	0.5	0.81	0.75	0.88	0.76	0.84	0.8	0.72	0.88	0.59
$\rho_r$	Beta	0.5	0.11	0.03	0.18	0.1	0.01	0.18	0.15	0.04	0.28
$\rho_p$	Beta	0.5	0.78	0.69	0.86	0.76	0.65	0.86	0.7	0.58	0.81
$\rho_w$	Beta	0.5	0.08	0.01	0.14	0.07	0.01	0.14	0.12	0.03	0.23
$\rho_{ga}$	Beta	0.5	0.51	0.39	0.63	0.5	0.34	0.66	0.52	0.37	0.67
$n_a$	Inv. Gamma	0.1	0.45	0.44	0.44	0.44	0.44	0.49	0.44	0.48	0.45
$n_b$	Inv. Gamma	0.1	0.19	0.25	0.21	0.22	0.17	0.27	0.2	0.15	0.25
$n_y$	Inv. Gamma	0.1	0.48	0.52	0.48	0.49	0.44	0.54	0.49	0.44	0.54
$n_h$	Inv. Gamma	0.1	0.36	0.41	0.35	0.35	0.29	0.42	0.34	0.28	0.4
$n_{ELB}^T$	Inv. Gamma	0.1	0.22	0.24	0.21	0.23	0.2	0.25	0.23	0.25	0.23
$n_{ELB}^F$	Gamma	0.03						0.01	0.02	0.02	0.03
$n_p$	Inv. Gamma	0.1	0.06	0.08	0.06	0.07	0.04	0.09	0.08	0.06	0.11
$n_{re}$	Inv. Gamma	0.1	0.37	0.41	0.37	0.37	0.32	0.41	0.35	0.3	0.4
$gain$	Gamma	0.035									
$1 - p_{11}$	Unif.	0.5									
$1 - p_{22}$	Unif.	0.5									
$\bar{\gamma}_{ELB}$	Normal	0.05									
Mode		-1112.17		-1043.00		-1041.5		-1010.1		-1024.9	
Laplace		-1194.87		1145.02		-1136.75		-1115.38		-1126.85	
MHM		-1194.72		-1145.12		-1144.11		-1112.19		-1123.188	
(log-) Bayes F.	1			21.54		21.97		35.87		31.09	

Table 3: Estimation period: 1966:I-2016:IV, exogenous switching models.

## 4.3 Learning Coefficients

Our simulation analysis in Section 2 suggests that regime switches, combined with sufficiently large gain values may lead to a jumping effect on some of the learning coefficients. In this section, we discuss the implied time-variation in our estimated learning models and check whether the jumping arises in some of the learning coefficients during the switch to the ELB period. Among the seven forward-looking variables, we focus on three variables that are characterized by relatively large changes during the crisis period and the subsequent switch to the ELB regime, namely asset prices  $q_t$ , consumption  $c_t$  and investment  $I_t$ . The general pattern is that the learning coefficients are more sensitive and more to the ELB switch under the AR(1) and LIL models, which is not surprising since the MSV model has the smallest estimated gain. Further, we observe that the learning process reacts to the crisis through different coefficients depending on the forecasting rule, which is discussed further below.

Figure 5 shows the perceived mean and persistence coefficients for the AR(1)-learning model, along with the corresponding 90% HPD intervals.<sup>30</sup> For all three variables, the perceived means jump down immediately following the crisis, which is more pronounced for asset prices and investment compared to consumption. For the perceived persistence parameters, there are sizeable upward jumps for asset prices and investment, while for consumption there is a smaller jump in the opposite direction. As such, the learning patterns for investment and asset prices, and to a smaller degree also consumption, show similarities to the simulation exercises in Section 2. The same results also hold labor  $l_t$  and rental rate of capital  $r_k t$  with upward jumps in perceived persistence and downward jumps in perceived mean, whereas for inflation and real wage these structural breaks do not arise since there are also no sharp changes in the data.<sup>31</sup>

Figure 6 shows a selected subset of the learning coefficients for the LIL model.<sup>32</sup> As mentioned above, the learning processes react differently depending on the forecasting rule, which already becomes visible by comparing the AR(1) and LIL models. Looking at the perceived mean parameters, it is readily seen that the drops during the crisis period are substantially smaller. However, looking at the second and third columns, we observe that the feedback from lagged interest rates and inflation jump. Particularly for lagged interest rate, the jumps are towards zero, suggesting a weakened impact from interest rates. Similarly the last column shows the feedback from lagged investment, which show the jumping pattern during the crisis period,

---

<sup>30</sup>In order to compute the HPD intervals for the learning coefficients, we use the final 20% of the MCMC sample for each model, which is further thinned with a factor 0.2, yielding a sample size of 10000 for the parameters. We then re-run the filter over these parameter draws to obtain the credible intervals for the learning coefficients.

<sup>31</sup>The corresponding figures for these variables are omitted for brevity.

<sup>32</sup>Similar to the AR(1) model, only a small portion of the learning coefficients are displayed given the size of the learning coefficient matrix.

although to a much smaller extent for the asset prices.<sup>33</sup>

Finally, Figure 7 shows some of the learning coefficients for the MSV-learning model. In this case, the largest change arises in the perceived mean coefficients, all of which start to rapidly decrease following the crisis. These variables show a disproportionately large response following the crisis, compared to their pre-crisis fluctuation levels. This large post-crisis response also helps to explain the small estimated gain in the MSV model. While a larger gain could generate more fluctuations pre-crisis and possibly improve the model fit, it would also make the post-crisis response substantially larger. The following two panels, similar to the LIL model, show the feedback from lagged interest rates and inflation respectively. In this case we observe more gradual responses rather than jumps, particularly for interest rates, which is not surprising given the small gain value. Nevertheless, we observe a similar change in direction for interest rates where the parameters move towards zero, suggesting a smaller impact from interest rates on these variables. The last column shows the perceived correlation parameters between the given variables and government spending process, which is of particular interest for the MSV model since the other two models assume unobserved shocks. We see that the perceived correlation moves away from zero for all three variables, suggesting a larger impact from an increased government spending. This is in line with the perceived weakened interest rate response, since it makes monetary policy less likely to offset any changes in government spending.

To see the effect of these changes in the perceived mean coefficients on the model fit, Figure 8 plots the in-sample forecasts for the growth rates of output, consumption, investment and wages for the MS-REE and all three learning model.<sup>34</sup> A known issue with REE models over the post-crisis period is the over-prediction of these growth rates: the sudden downward shift in the interest rates implies an increase in the growth rates of the model variables, whereas in fact the growth rates have been slightly lower than the pre-crisis historical averages for output, consumption and investment. As a consequence, the models tend to over-predict these variables if no additional structural break is introduced into the model. Figure 8d shows that this is indeed the case under MS-REE for the growth rates of output, consumption and investment. As opposed to this, Panels a-c in Figure 8 show that this over-prediction issue does not arise in the learning models. We interpret this downward shift in the learning models as a consequence of the time-variation in the learning coefficients. Accordingly, the lower growth rates over the post-crisis period emerge as a simple consequence of a pessimistic wave reflected in the perceived mean coefficients.

---

<sup>33</sup>Note that we omit the learning coefficients on own lagged variables with the exception of investment: the lagged asset price is not present in the learning matrix, and the response of consumption to lagged consumption does not show a meaningful change over the relevant period.

<sup>34</sup>Hence, these plots simply break down the log-likelihood of each model to period-specific increments.

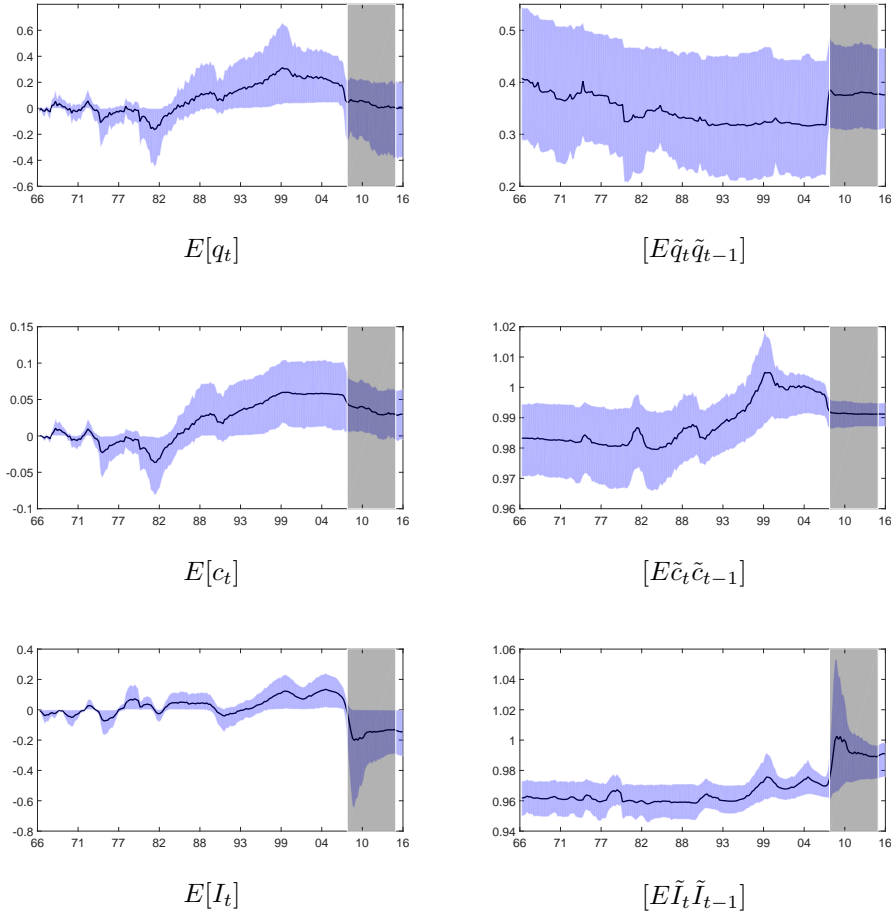


Figure 5: Selected learning coefficients: AR(1) model.  $q_t$ ,  $c_t$  and  $I_t$  denote asset prices, consumption and investment respectively, whereas  $\tilde{q}_t$ ,  $\tilde{c}_t$  and  $\tilde{I}_t$  denote their demeaned counterparts. The shaded area corresponds to 2008Q4-2015Q1, which is the period where all models agree that the ELB constraint is binding.

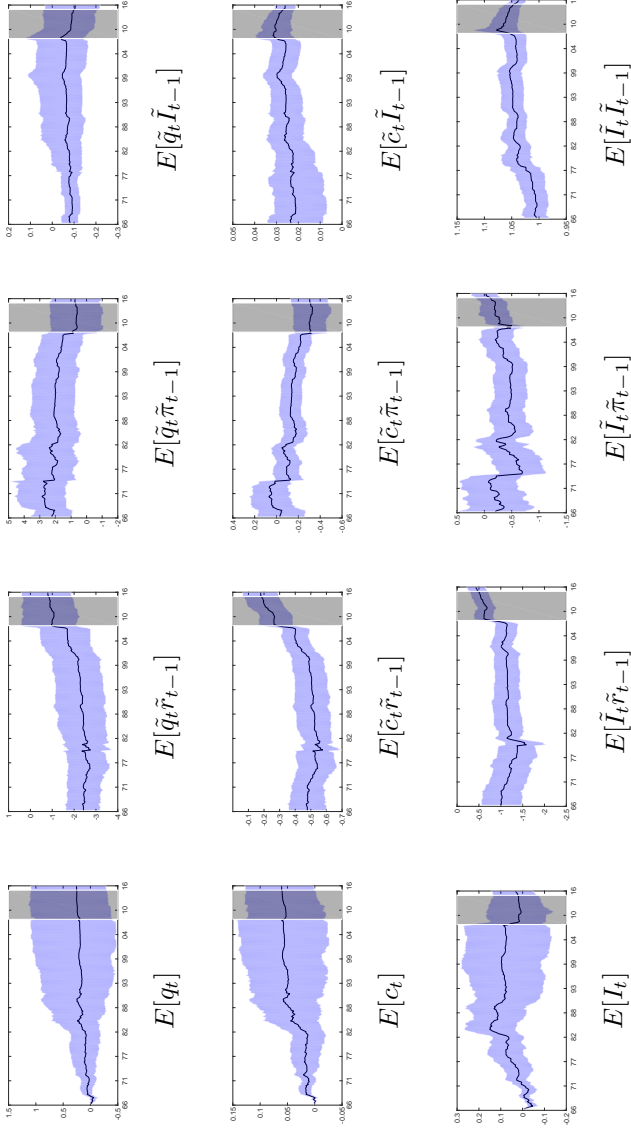


Figure 6: Selected learning coefficients: LIL model.  $q_t$ ,  $c_t$ ,  $I_t$ ,  $r_t$  and  $\pi_t$  denote asset prices, consumption, investment, nominal interest rates and inflation respectively, and the variables with a tilde denote their demeaned counterparts. The shaded area denotes the period 2008Q4-2015Q1

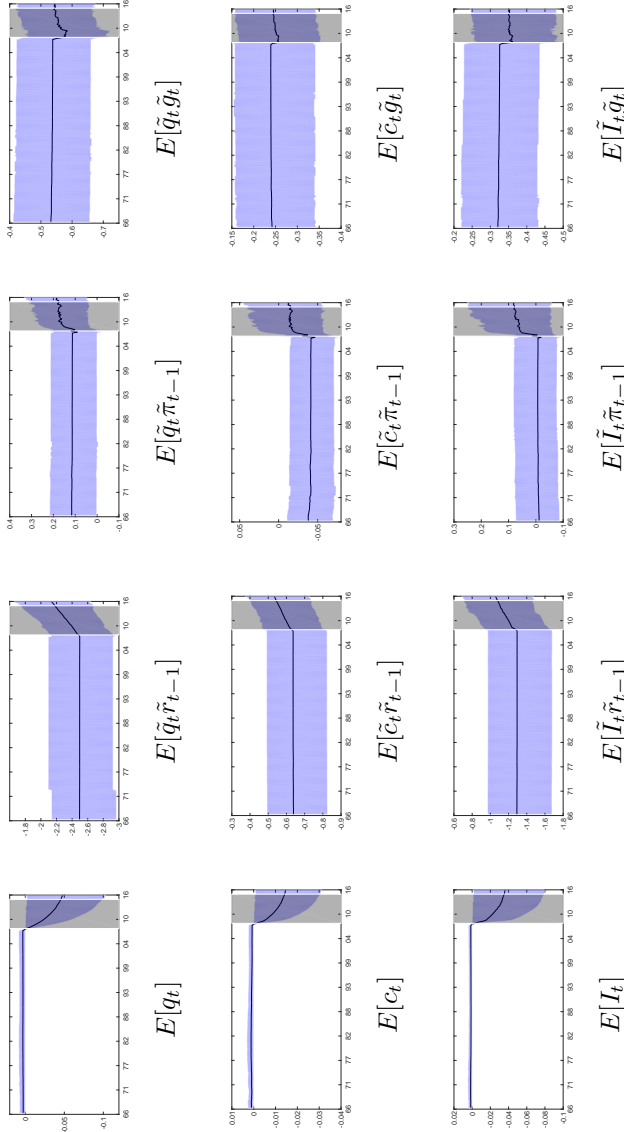


Figure 7: Selected learning coefficients: MSV model.  $q_t$ ,  $c_t$ ,  $I_t$ ,  $r_t$ ,  $\pi_t$  and  $g_t$  denote asset prices, consumption, investment, nominal interest rates, inflation and government spending process respectively, and the variables with a tilde denote their demeaned counterparts. The shaded area denotes the period 2008Q4-2015Q1

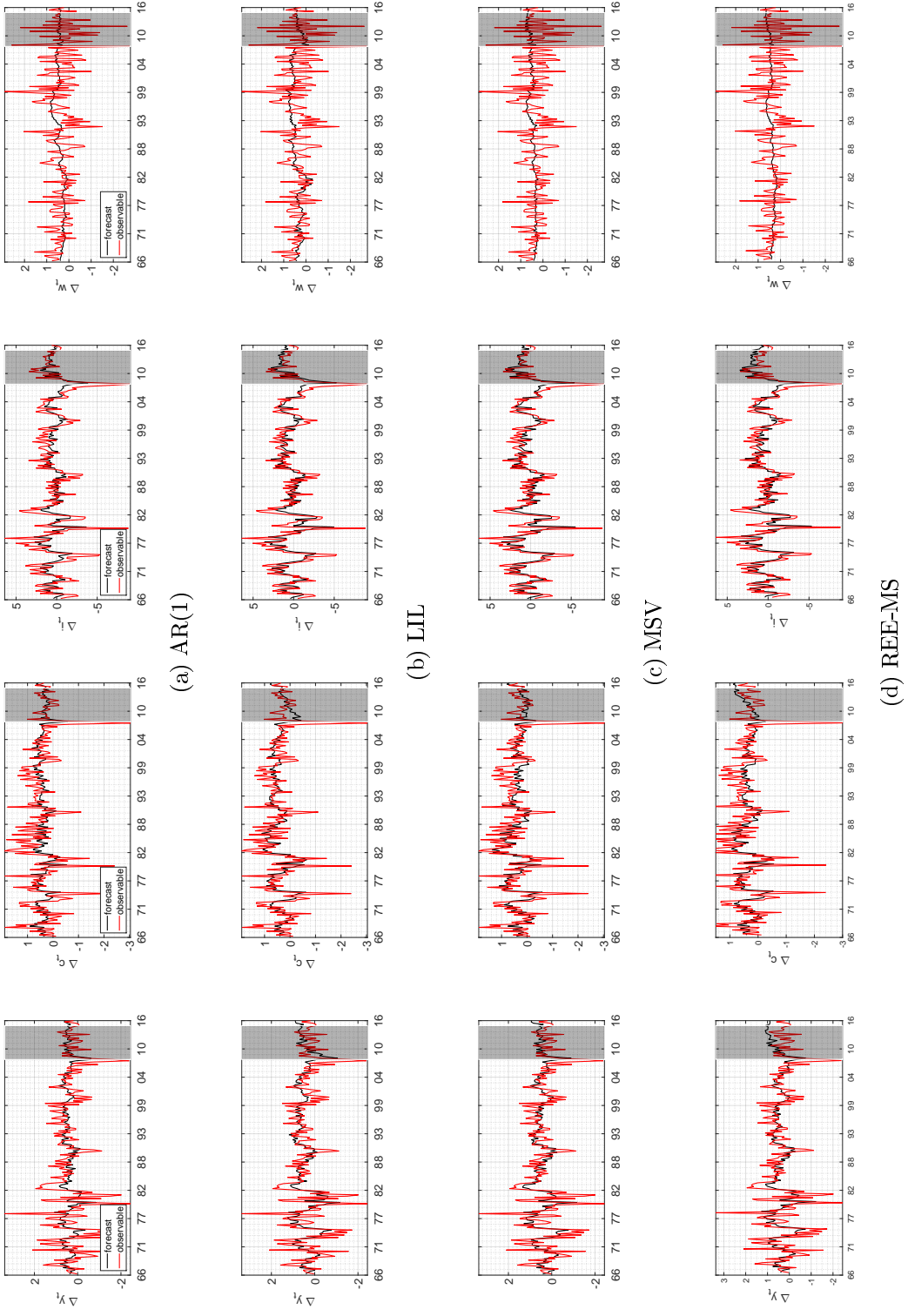


Figure 8: In-sample forecasts (obtained from the forecasting step of the filter) for the growth rates. From left to right: output growth  $\Delta y_t$ , consumption growth  $\Delta c_t$ , investment growth  $\Delta i_t$  and wage growth  $\Delta w_t$ . The shaded area denotes the period 2008Q4-2015Q1

## 4.4 Impulse Responses

Having established the differences between the MS-REE and learning models in terms of the model fit, estimated parameters and learning coefficients, we next discuss some of the impulse response functions (IRFs) between learning and REE-MS. For the learning models, we focus on the period specific conditional IRFs over 2002Q1-2016Q4, which are presented in Figure 9 for output. The black and red lines at the left- and right-most sides correspond to the impulse responses for the REE-MS model under the normal and ELB regimes respectively. We focus on four shocks, namely the productivity  $\eta_a$ , risk premium  $\eta_b$ , government spending  $\eta_g$  and price mark-up  $\eta_p$ . For the learning models, the IRFs during the period 2008Q4-2015Q1 are computed under the ELB regime, while the remaining IRFs are computed under the normal regime.<sup>35</sup>

The learning IRFs are characterized by two jumps in 2008 and 2015, which correspond to the ELB entry and exit periods. The jumps show that there are large differences between the IRFs calculated under the normal and ELB regimes. The overall time variation before and after the crisis is different for each model. For the AR(1) model in the first panel, the time variation for all shocks is relatively small compared to the jump in 2008. For the LIL model, there is more time variation after the crisis period. In particular for productivity and government spending shocks, the IRFs gradually move in the direction of the REE-MS (i.e. the red line), until the system switches back to the normal regime in 2015. For the MSV-learning model, we observe a gradual movement towards REE-MS impulse response during the ELB regime. These patterns reveal that the learning process manifests itself in the IRFs as a slow convergence towards the REE-MS model for the LIL and MSV models. As such, the learning and rational models generate different impulse responses at the beginning of the ELB regime, where the difference slowly diminishes as the system spends more time in the ELB regime. In Appendix D, we show that a similar pattern is also present in the IRFs of consumption and investment for the learning models.

A second important point related to IRFs is the difference between regime specific impulse responses for learning and REE-MS models: the difference between regime-specific impulse responses under REE-MS models (i.e. the difference between black and red lines) is typically larger than the difference for learning models. To examine this more formally, we consider the following exercise: we take five year periods during the normal regime before the crisis (2002:I-2006:IV) and during the ELB regime after the crisis (2010:I-2014:IV). For the learning models, we compute the median differences in the impulse responses between the two regimes, along with the minimum and maximum differences in the IRFs to serve as a pseudo confidence interval

---

<sup>35</sup>In other words, we ignore the minor differences between the estimated regime probabilities during the ELB entry and exit for the learning models. Alternatively, we can compute the IRFs under both regimes and average them using the estimated regime probabilities. While this generates nearly identical results, it mixes up the effects of learning and regime uncertainty during the transition period.

for these differences. Figure 10 plots these IRF differentials, along with the corresponding difference under REE-MS case. What becomes quickly evident is that, the differences in learning models are smaller than the differences in the REE model in a majority of the cases: with the exception of the risk premium shock in LIL and MSV models, the black line (learning model) and the associated pseudo confidence interval remains below the blue line (REE model). This result suggests that the REE-MS model overestimates the impact of the ELB regime on the propagation of shocks, relative to the learning models.

An implication of these differences in impulse responses is on fiscal multipliers: a standard finding with the REE models is that fiscal multipliers are typically larger when the ELB constraint is binding, compared to when it is not binding. Figure 11 shows the regime-specific cumulative fiscal multipliers for the REE-MS and all three learning models.<sup>36</sup> All learning models confirm that there is an increase in the fiscal multiplier at the ELB regime, but the magnitudes are different. Over a 10-year period, the REE-MS model implies that the cumulative multiplier is up to 3.5 times larger in the ELB regime, compared to the normal regime. For the LIL and MSV-learning models, the ratio remains similar to the REE-MS model up to 12 quarters, after which it remains below the REE-MS ratio over all horizons: for the LIL model, the ratio reaches a maximum of 3, while for the MSV-learning model the maximum ratio is around 2.5. For the AR(1) model, the ratio is even smaller, with a maximum ratio staying below 2. These results imply that the impact of the ELB constraint on fiscal multipliers is different under learning models: while the short-term effects are ambiguous, the multipliers are uniformly smaller under all learning models over longer horizons.

## 4.5 Posterior Results: Endogenous Switching Models

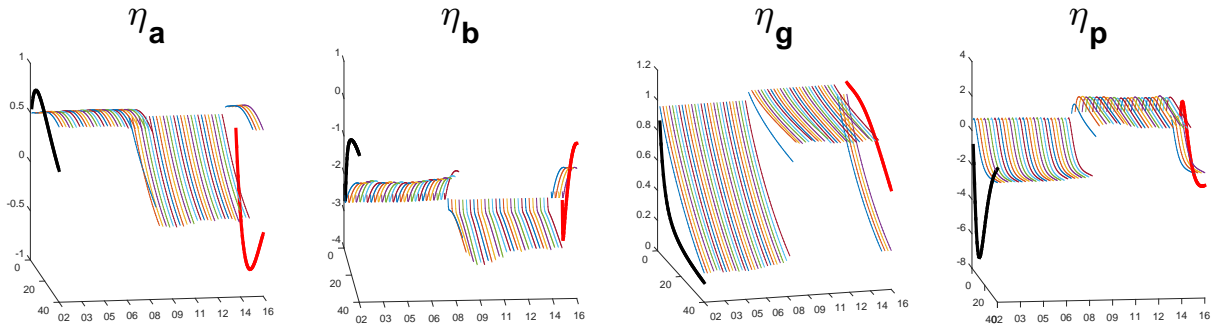
In this section, we discuss the estimation results of the learning models with endogenous switching. While this does not lead to important changes in terms of the estimation results and parameter values, the presence of endogenous transition probabilities serve as an important stepping stone for the counterfactual simulations that we consider in Section 4.6. We define the transition probabilities for the normal and ELB regimes as follows:

$$p_{11}(t) = \frac{\theta}{\theta + \exp(-\phi_T(i_t^* - \bar{i}^*))}, \quad p_{22}(t) = \frac{\theta}{\theta + \exp(\phi_{ELB}(i_t^* - \bar{i}^*))},$$

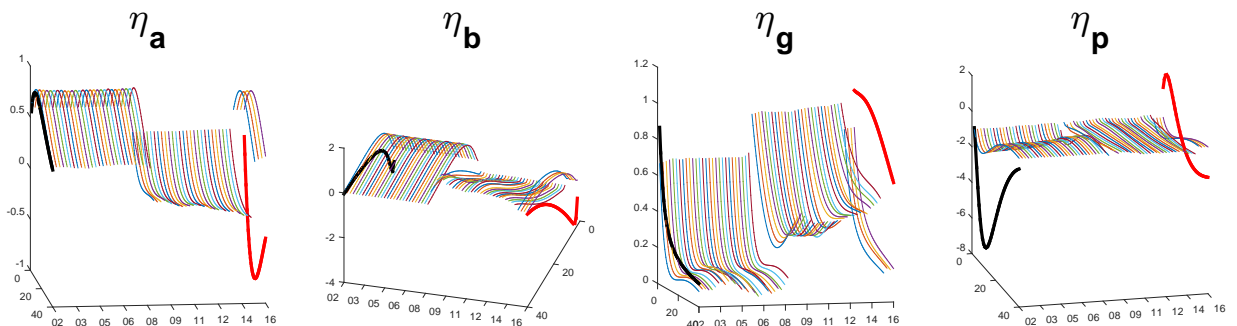
with  $1 - p_{11}$  the exit probability from the normal regime, and  $1 - p_{22}$  the exit probability from the ELB regime.  $i_t^*$  denotes the shadow rate, defined as follows:

---

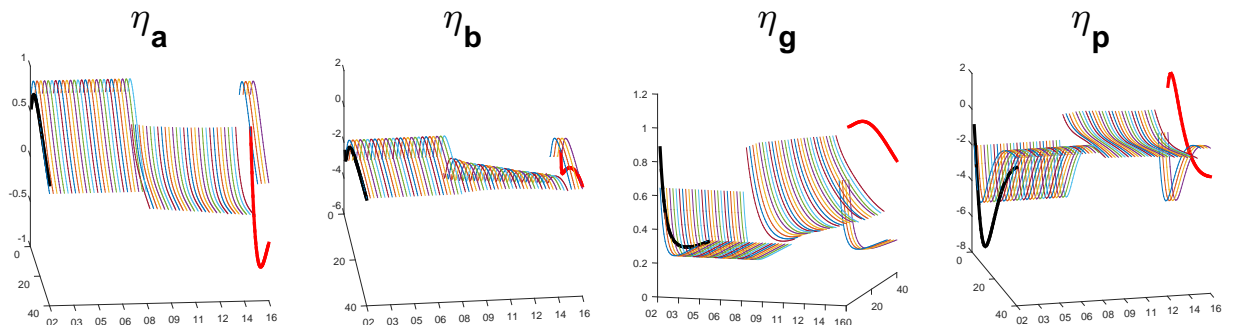
<sup>36</sup>The fiscal multiplier is computed as  $FM = \frac{\sum_{i=1}^N \frac{\partial y_i}{\partial \eta_g}}{\sum_{i=1}^N \frac{\partial g_i}{\partial \eta_g}}$ , i.e. the cumulative response of output to a one standard deviation shock, divided by the cumulative response of government spending process over the same period. In the figures we set  $N = 40$ , which yields multipliers up to 10 years.



(a) AR(1)

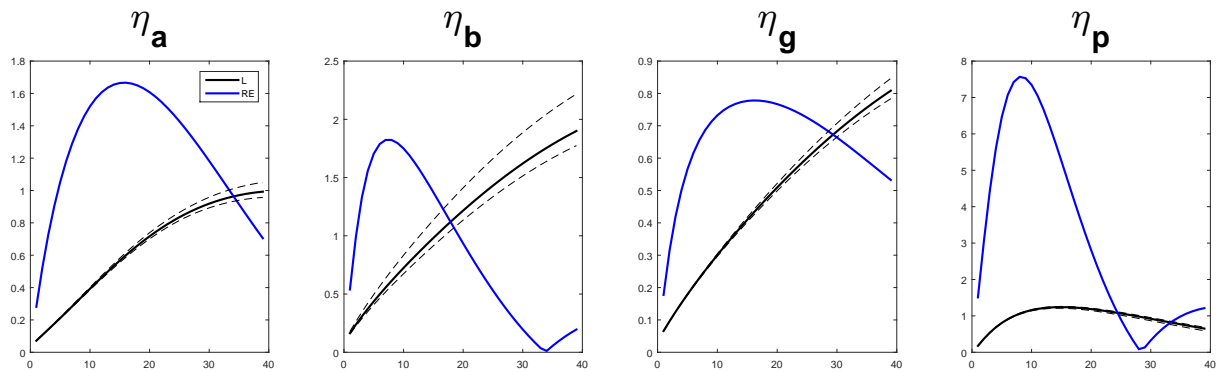


(b) LIL

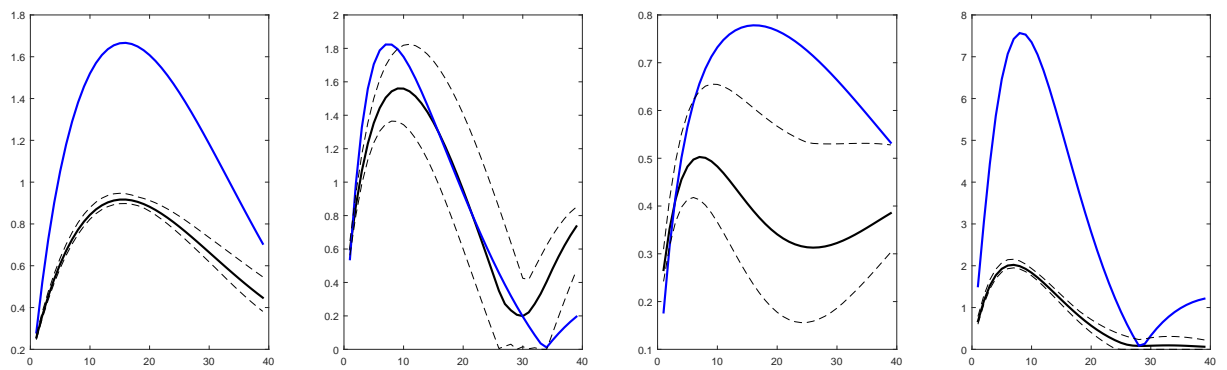


(c) MSV

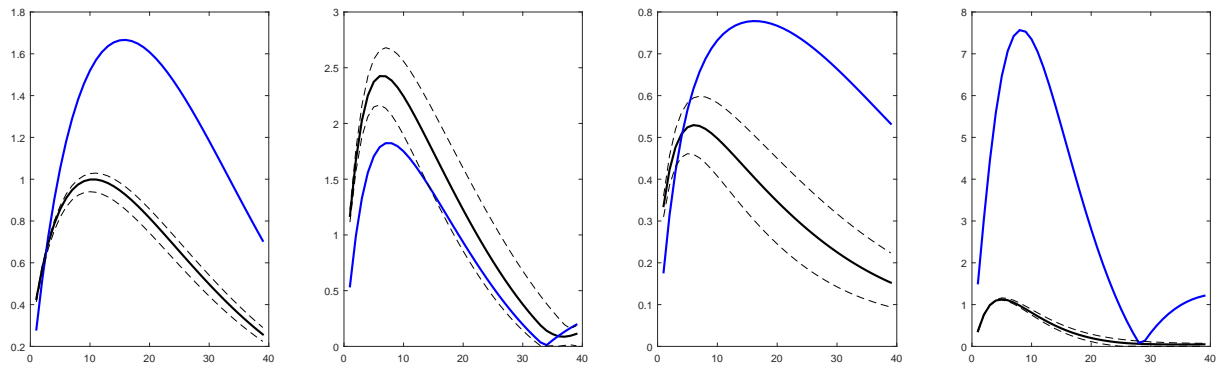
Figure 9: **Output:** Comparison of learning IRFs with REE IRFs. Each IRF shows a one standard deviation shock of  $\eta_a, \eta_b, \eta_g, \eta_p$  respectively.



(a) AR(1)



(b) LIL



(c) MSV

Figure 10: **Output:** Impulse response differentials between normal and ELB regimes.

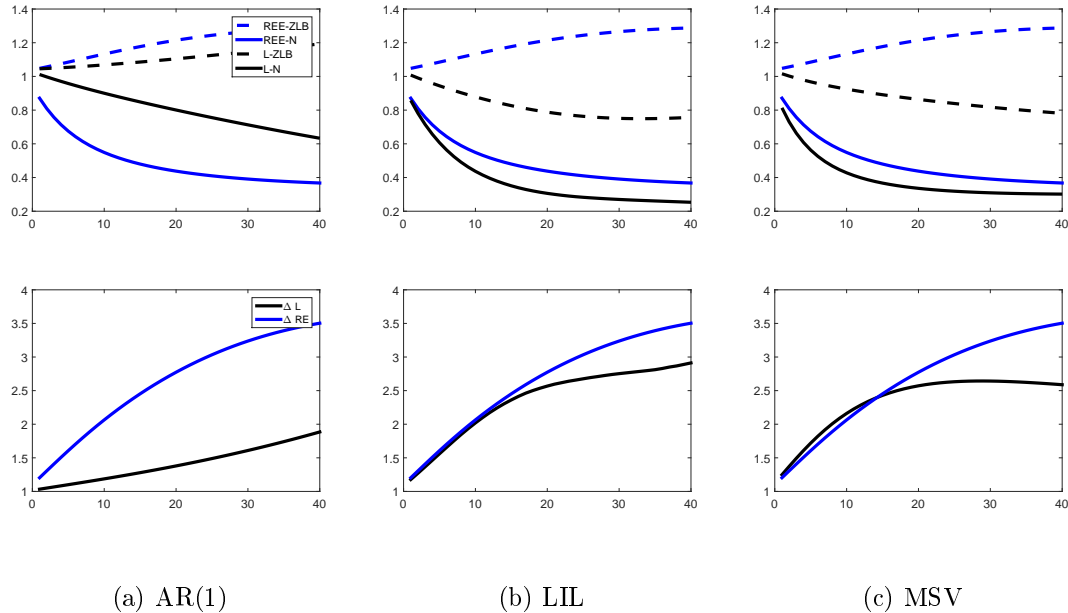


Figure 11: Comparison of cumulative fiscal multiplier ratios between REE and learning models over the normal and ELB regimes.

$$i_t^* = \rho i_{t-1}^* + (1 - \rho)(\phi_\pi \pi_t + \phi_x x_t) + \phi_{\Delta x} \Delta x_t.$$

This equation defines the shadow rate as the interest rate that would prevail in the absence of monetary policy shocks and the ELB constraint. According to our transition functions, the probability of entering the ELB regime increases as the shadow rate approaches zero or falls below zero. In our estimations, we fix the first hyperparameter  $\theta = 1$ , and estimate the second hyperparameter for each regime,  $\phi_T$  and  $\phi_{ELB}$ , using a Gamma prior with mean 0.2 and standard deviation 0.1. The parameter determines the shape of the transition function: large values lead to a sharp change in the transition probability as interest rates get close to zero, while low values lead to a more gradual change in the transition probability.

Tables 4 and 5 show the estimation results for all three learning models. For the LIL and MSV-learning models, the marginal likelihood is better compared to their exogenous switching counterparts, while for the AR(1) model there is no discernible difference. For the hyperparameters of the transition probabilities, the entry and exit parameters remain fairly close to each other. For the AR(1) model, the parameter on exiting the normal regime is lower at 0.1 compared to the ELB parameter at 0.18, which suggests that the ELB entry function is smoother than the ELB exit function. Nevertheless, these two parameters have relatively large HPD bands covering both sharp and smooth cases of the transition functions, suggesting that the exact shape of the function is not well identified for the transition to and from the ELB

regime.

Table 6 shows the estimated regime probabilities, along with the estimated shadow rates. Compared with the exogenous switching models, we observe that the regimes are estimated with more certainty, since the regime probabilities are estimated at 0% or 100% in the endogenous switching case. During the ELB entry, we observe a similar pattern across the learning models compared to the exogenous switching case: the AR(1) model enters the ELB regime from 2008Q4 onwards, while the LIL and MSV models enter the regime from 2008Q3 onwards. As such, 2008Q3 is the only period with disagreement among the models, and they all agree that the system is in the ELB regime from 2008Q4 onwards.

During the exit, we again observe similar differences between the models compared to the exogenous switching case. While the AR(1) model generates a return to the normal regime from 2015Q2 onwards, the MSV and LIL models remain in the ELB regime until the end of our sample period. As such, the only difference during the exit between the endogenous and exogenous switching cases arises in the LIL model, which showed a pattern similar to the AR(1) model in the previous case.

The patterns observed in the estimated shadow rates are consistent with the estimated regime probabilities. It is readily seen that the AR(1) model is characterized by higher shadow rates both during the crash in 2008, and after the recovery in 2015. As a result, while the shadow rate under the AR(1) model returns to positive levels by the end of the sample, the rates under LIL and MSV models are still in the negative domain. As already discussed in the exogenous switching section, the observed differences in the shadow rates are a result of both the estimated Taylor rule parameters, as well as the differences in the filtered output gap processes. The AR(1) model predicts a smaller drop in the output gap process compared to the other two models.<sup>37</sup> This is combined with a higher interest rate smoothing parameter (and therefore a smaller initial reaction) that leads to a smaller drop in the estimated shadow rate. Similar to the exogenous switching models, we do not disentangle these effects further, but rather interpret the differences as the uncertainty surrounding the ELB exit period.

To illustrate the results, Figure 12 shows the estimated shadow rate for the AR(1) model for the last 15 years of the sample, from 2001Q1 onwards. The implied time path of the shadow rate and the transition functions for the other two models look fairly similar, which are omitted here.<sup>38</sup> We use the endogenous switching models to consider a set of counterfactual simulations over the ELB period in the next section.

---

<sup>37</sup>The differences in the output gap processes in turn are due to differences in the filtered productivity processes. A smaller drop in productivity in the AR(1) model leads to a smaller drop in the output gap process.

<sup>38</sup>One difference between the AR(1) model and the other two learning models, as already discussed, is that the shadow rate is characterized by a smaller drop in the AR(1) model during the entry to the ELB regime. Other than this difference in levels, the implied pattern in the shadow rates is similar across the models.

Para	Prior	MSV			LIL			AR(1)		
		Dist	Mean	HPD 90%	Mean	HPD 90%	Mean	HPD 90%	Mean	HPD 90%
$\phi$	Normal	4	5.26	3.39	7.23	5.03	3.41	6.76	4.7	2.93
$\sigma_c$	Normal	1.5	1.17	0.98	1.37	1.12	1.03	1.21	1.05	0.59
$\lambda$	Beta	0.7	0.75	0.67	0.84	0.82	0.76	0.88	0.78	0.67
$\xi_w$	Beta	0.5	0.93	0.9	0.95	0.84	0.76	0.91	0.76	0.68
$\sigma_l$	Normal	2	2.14	0.83	3.53	2.66	1.5	3.85	1.99	0.76
$\xi_p$	Beta	0.5	0.79	0.74	0.84	0.75	0.68	0.82	0.78	0.7
$t_w$	Beta	0.5	0.81	0.68	0.94	0.7	0.49	0.91	0.51	0.28
$\iota_p$	Beta	0.5	0.12	0.03	0.23	0.34	0.16	0.53	0.27	0.1
$\psi$	Beta	0.5	0.61	0.41	0.78	0.56	0.36	0.77	0.54	0.29
$\phi_p$	Normal	1.25	1.55	1.41	1.69	1.57	1.43	1.71	1.54	1.4
$r_\pi$	Normal	1.25	1.81	1.51	2.1	1.48	1.09	1.88	1.63	1.19
$\rho$	Beta	0.75	0.86	0.82	0.89	0.86	0.82	0.91	0.95	0.93
$r_y$	Normal	0.125	0.12	0.08	0.17	0.14	0.09	0.18	0.06	0.01
$r_{\Delta y}$	Normal	0.125	0.2	0.16	0.23	0.18	0.14	0.22	0.16	0.13
$\bar{\pi}$	Gamma	0.625	0.75	0.59	0.93	0.67	0.48	0.88	0.69	0.48
$\bar{\beta}$	Gamma	0.25	0.18	0.07	0.29	0.17	0.06	0.29	0.19	0.06
$\bar{l}$	Normal	0	1.91	0.63	3.12	1.88	0.12	3.56	0.58	-1.22
$\bar{\gamma}$	Normal	0.4	0.41	0.39	0.44	0.42	0.39	0.45	0.4	0.36
$\alpha$	Normal	0.3	0.17	0.14	0.2	0.18	0.15	0.21	0.16	0.12
Mode			-1045.1			-1008.3			-1026.2	
Laplace			-1154.07			-1116.51			-1125.76	
MHM			-1134.25			-1108.17			-1123.32	
(Log-) Bayes F.			26.26			37.59			31.01	

Table 4: Estimation period: 1966:I-2016:IV, endogenous switching models.

Para	Prior	Dist	MSV			LIL			AR(1)		
			Mean	HPD 90%	Mean	HPD 90%	Mean	HPD 90%	Mean	HPD 90%	Mean
$\rho_a$	Beta	0.5	0.94	0.91	0.97	0.97	0.95	0.98	0.96	0.93	0.99
$\rho_b$	Beta	0.5	0.43	0.24	0.63	0.26	0.14	0.37	0.33	0.2	0.46
$\rho_g$	Beta	0.5	0.98	0.97	0.99	0.98	1	0.98	0.96	0.96	1
$\rho_i$	Beta	0.5	0.8	0.72	0.87	0.61	0.5	0.72	0.5	0.38	0.63
$\rho_r$	Beta	0.5	0.12	0.03	0.22	0.23	0.08	0.38	0.11	0.02	0.2
$\rho_p$	Beta	0.5	0.7	0.57	0.82	0.07	0.01	0.16	0.05	0.01	0.11
$\rho_w$	Beta	0.5	0.12	0.02	0.22	0.15	0.04	0.27	0.1	0.01	0.2
$\rho_{ga}$	Beta	0.5	0.51	0.35	0.67	0.53	0.37	0.69	0.51	0.36	0.66
$\eta_a$	Inv. Gamma	0.1	0.44	0.39	0.49	0.45	0.4	0.5	0.45	0.4	0.51
$\eta_b$	Inv. Gamma	0.1	0.2	0.15	0.25	0.3	0.27	0.33	0.3	0.26	0.34
$\eta_g$	Inv. Gamma	0.1	0.49	0.44	0.54	0.49	0.45	0.55	0.48	0.44	0.53
$\eta_i$	Inv. Gamma	0.1	0.34	0.28	0.4	0.81	0.73	0.89	0.78	0.7	0.86
$\eta_r^T$	Inv. Gamma	0.1	0.23	0.2	0.26	0.23	0.21	0.26	0.22	0.2	0.25
$\eta_r^{ELB}$	Gamma	0.03	0.03	0.02	0.03	0.02	0.02	0.03	0.01	0.01	0.01
$\eta_p$	Inv. Gamma	0.1	0.08	0.05	0.11	0.11	0.08	0.15	0.07	0.04	0.11
$\eta_w$	Inv. Gamma	0.1	0.35	0.3	0.4	0.4	0.36	0.44	0.38	0.34	0.42
$gain$	Gamma	0.035	0.0011	0.0001	0.0026	0.0047	0.0013	0.0084	0.0046	0.0001	0.010
$\bar{\gamma}^{ELB}$	Normal	0.05	0.04	0.03	0.05	0.04	0.03	0.05	0.03	0.03	0.04
$\frac{\Phi_T}{1000}$	Gamma	0.2	0.17	0.03	0.38	0.19	0.03	0.39	0.1	0.01	0.25
$\frac{\Phi_{ZLB}}{1000}$	Gamma	0.2	0.2	0.05	0.38	0.21	0.04	0.4	0.18	0.03	0.36
Mode		-1045.1			-1008.3				-1026.2		
Laplace		-1154.07			-1116.51				1125.76		
MHM		-1134.25			-1108.17				-1123.32		
(Log-) Bayes F.		26.26			37.59				31.01		

Table 5: Estimation period: 1966:I-2016:IV, endogenous switching models.

Date	Model					
	AR(1)		LIL		MSV	
	ELB prob.	Shadow rate	ELB prob.	Shadow rate	ELB prob.	Shadow rate
08Q3	0%	0.78	0%	0.4	0%	0.36
08Q3	0%	0.37	100%	-0.12	100%	-0.21
08Q4	100%	-0.27	100%	-0.92	100%	-1.06
09Q1	100%	-0.64	100%	-1.43	100%	-1.58
15Q2	100%	-0.01	100%	-1.15	100%	-1.02
15Q2	0%	0.05	100%	-1.12	100%	-0.99
15Q3	0%	0.04	100%	-1.10	100%	-0.96

Table 6: Estimated average ELB regime probabilities and shadow rates in endogenous switching models.

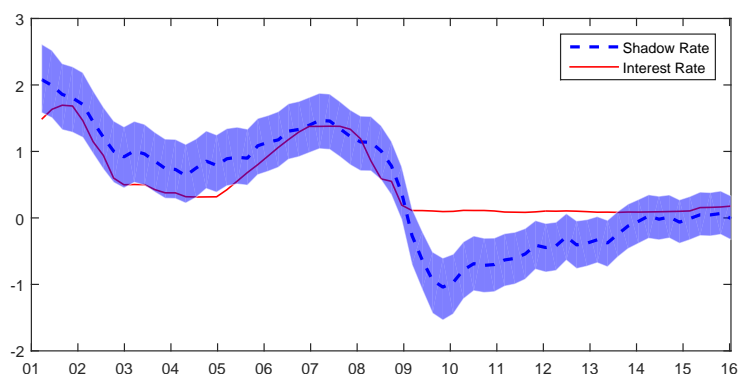


Figure 12: Nominal interest rate and the estimated shadow rate over the sample period for the AR(1) model.

## 4.6 Counterfactual Simulations

In this section we investigate the impact of learning dynamics on the ELB duration through a set of counterfactual experiments. We consider the following setup with the estimated endogenous switching models: using the MCMC draws for the learning models, we first run the filter up to period 2008Q4. From 2008Q4 onwards, we simulate the economy for a period of 8 years (32 quarters). For each model, we use a total of 1000 MCMC draws, where the parameter draws are taken from the last 20 % of the MCMC simulation with a thinning factor of 0.02. We repeat this exercise for each learning model under the estimated gain value, as well as different gain values to isolate and assess the effects of learning on the ELB duration.

Figure 13 shows the average ELB exit probabilities for five experiments with gain values between 0 and 0.0075, along with the benchmark experiment with the estimated gain value. This exercise reveals a clear pattern where smaller gain values are associated with higher average exit probabilities. In all three models, the case with no updating ( $gain = 0$ ) yields the largest exit probability, while the case with the most updating ( $gain = 0.0075$ ) yields the lowest exit probability. The magnitude of changes in these probabilities differs across the models: the exit probabilities oscillate in the range 50%-70% in the AR(1) model, 25%-95% in the LIL model and 57%-99% in the MSV model. Nevertheless, they all point in the same direction where a faster learning process leads to a worse outcome and a prolonged ELB episode.<sup>39</sup>

In light of the above results, there are several key takeaways from this section. First and foremost, our results indicate that the presence of stronger learning dynamics unambiguously increase the frequency of long-lived ELB regimes. This offers two potential interpretations for the 2008-2015 period through the lens of our learning models. The first one is that expectations may have been well anchored during this period and the effects of learning were limited. Second, while learning dynamics created a downward pressure on the economy, there were other channels at play that may have offset the adverse effects of learning. In particular, unconventional monetary policy tools such as forward guidance and quantitative easing might have had such an impact. Importantly, a potential anchoring of expectations and the effects of unconventional policy are not mutually exclusive events. We leave an exploration of policy interactions with expectations under learning to future research.

## 5 Conclusions

In this paper we explored a general regime switching setup subject to adaptive learning, where the agents' do not know the full details of a complex economy, and use past data to update

---

<sup>39</sup> Appendix F provides some additional figures on the distribution of ELB regime durations, and time paths of inflation and output gap over the counterfactual period for all learning models.

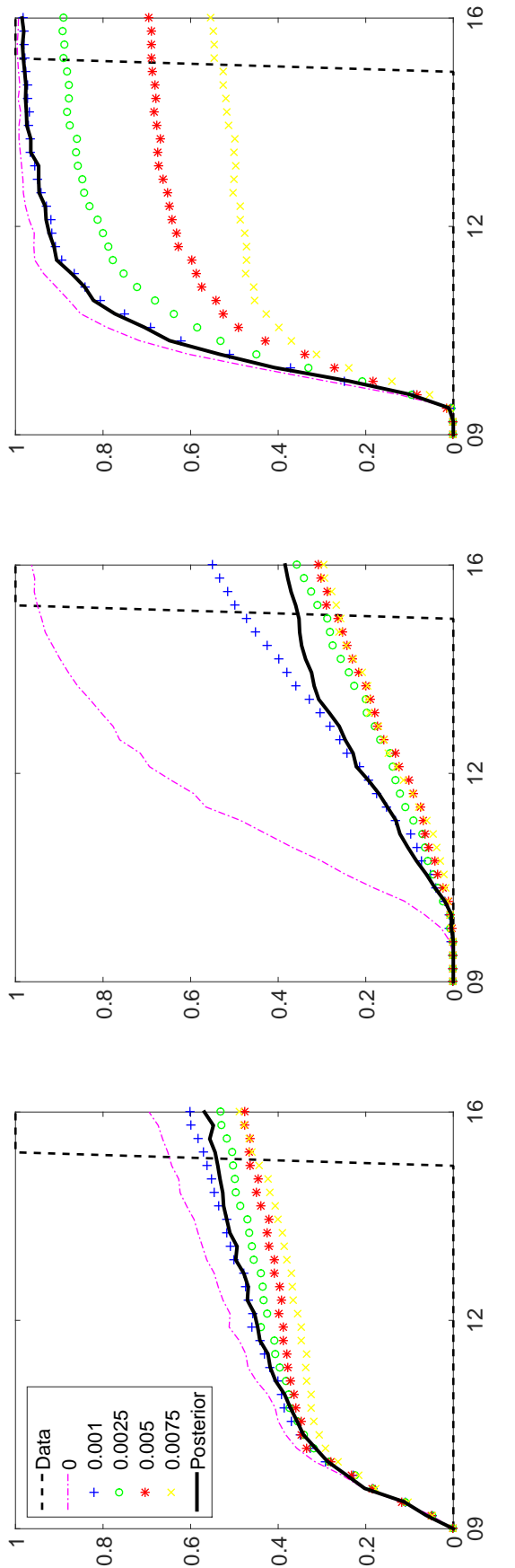


Figure 13: Average ELB exit probabilities in learning models under different counterfactual scenarios. We use five different gain values between [0, 0.0075] to isolate the effects of learning in each model. The averages are obtained from 1000 simulations in each scenario, where the parameter values are taken from the posterior distributions.

their models and form their expectations about the future. We provided an estimation method to handle this class of models, and applied it to the Smets-Wouters (2007) model over the ELB period during 2008–2015. Our results show that adaptive learning models generally improve the model fit relative to the REE benchmarks. We find that impulse responses under REE and adaptive learning models typically move in the same direction once the economy switches to the ELB regime. However, the magnitudes of the changes tend to be smaller and more gradual under adaptive learning, which suggests that standard REE models might overestimate the impact of the ELB on the propagation of shocks. Our counterfactual experiments reveal that stronger learning effects over the ELB episode tend to put a downward pressure on the economy and prolong the duration of the ELB regime. This suggests that other effects, such as unconventional policy tools and in particular forward guidance, might have had an offsetting effect on learning dynamics over this period. We leave an explicit analysis of the relation between adaptive learning and unconventional monetary policy to future research.

## References

- Adjemian, S., Bastani, H., Juillard, M., Mihoubi, F., Perendia, G., Ratto, M., & Villemot, S. (2011). Dynare: Reference manual, version 4.
- Airaudo, M. & Hajdini, I. (2019). Regime switching consistent expectations equilibria: General results with application to monetary policy.
- Anufriev, M., Hommes, C., & Makarewicz, T. (2019). Simple forecasting heuristics that make us smart: Evidence from different market experiments. *Journal of the European Economic Association*, 17(5), 1538–1584.
- Arifovic, J., Schmitt-Grohé, S., & Uribe, M. (2018). Learning to live in a liquidity trap. *Journal of Economic Dynamics and Control*, 89, 120–136.
- Berardi, M. & Galimberti, J. K. (2017a). Empirical calibration of adaptive learning. *Journal of Economic Behavior & Organization*, 144, 219–237.
- Berardi, M. & Galimberti, J. K. (2017b). On the initialization of adaptive learning in macroeconomic models. *Journal of Economic Dynamics and Control*, 78, 26–53.
- Berardi, M. & Galimberti, J. K. (2017c). Smoothing-based initialization for learning-to-forecast algorithms. *Macroeconomic Dynamics*, (pp. 1–16).
- Bianchi, F. (2016). Methods for measuring expectations and uncertainty in markov-switching models. *Journal of Econometrics*, 190(1), 79–99.

Bianchi, F. & Ilut, C. (2017). Monetary/fiscal policy mix and agents' beliefs. *Review of economic Dynamics*, 26, 113–139.

Bianchi, F. & Melosi, L. (2017). Escaping the great recession. *American Economic Review*, 107(4), 1030–58.

Binning, A. & Maih, J. (2016). Implementing the zero lower bound in an estimated regime-switching dsge model.

Bonam, D., de Haan, J., Soederhuizen, B., et al. (2017). *The effects of fiscal policy at the effective lower bound*. Technical report, Netherlands Central Bank, Research Department.

Branch, W. A., Davig, T., & McGough, B. (2013). Adaptive learning in regime-switching models. *Macroeconomic Dynamics*, 17(5), 998–1022.

Bullard, J. & Duffy, J. (2004). Learning and structural change in macroeconomic data. *FRB of St. Louis Working Paper No.*

Bullard, J. & Eusepi, S. (2014). When does determinacy imply expectational stability? *International Economic Review*, 55(1), 1–22.

Bullard, J. & Mitra, K. (2002). Learning about monetary policy rules. *Journal of monetary economics*, 49(6), 1105–1129.

Busetti, F., Ferrero, G., Gerali, A., & Locarno, A. (2014). Deflationary shocks and de-anchoring of inflation expectations. *Bank of Italy Occasional Paper*, (252).

Chen, H. (2017). The effects of the near-zero interest rate policy in a regime-switching dynamic stochastic general equilibrium model. *Journal of Monetary Economics*, 90, 176–192.

Chung, H. & Xiao, W. (2013). *Cognitive consistency, signal extraction, and macroeconomic persistence*. Technical report, mimeo, SUNY Binghamton.

Davig, T. & Leeper, E. M. (2007). Generalizing the taylor principle. *American Economic Review*, 97(3), 607–635.

Di Pace, F., Mitra, K., & Zhang, S. (2016). Adaptive learning and labour market dynamics.

Eusepi, S. & Preston, B. (2011). Expectations, learning, and business cycle fluctuations. *American Economic Review*, 101(6), 2844–72.

Evans, G. W., Guse, E., & Honkapohja, S. (2008). Liquidity traps, learning and stagnation. *European Economic Review*, 52(8), 1438–1463.

Evans, G. W. & Honkapohja, S. (2010). 11 expectations, deflation traps and macroeconomic policy. *Twenty Years of Inflation Targeting: Lessons Learned and Future Prospects*, (pp. 232).

Evans, G. W. & Honkapohja, S. (2012). *Learning and expectations in macroeconomics*. Princeton University Press.

Farmer, R. E., Waggoner, D. F., & Zha, T. (2009). Understanding markov-switching rational expectations models. *Journal of Economic theory*, 144(5), 1849–1867.

Farmer, R. E., Waggoner, D. F., & Zha, T. (2011). Minimal state variable solutions to markov-switching rational expectations models. *Journal of Economic Dynamics and Control*, 35(12), 2150–2166.

Gaus, E. & Gibbs, G. C. (2018). *Expectations and the empirical fit of DSGE models*. Technical report, Mimeo.

Gelman, A., Rubin, D. B., et al. (1992). Inference from iterative simulation using multiple sequences. *Statistical science*, 7(4), 457–472.

Geweke, J. (1992). Evaluating the accuracy of sampling-based approaches to the calculations of posterior moments. *Bayesian statistics*, 4, 641–649.

Gust, C., Herbst, E., & Lopez-Salido, J. D. (2018). Forward guidance with bayesian learning and estimation.

Hollmayr, J. & Matthes, C. (2015). Learning about fiscal policy and the effects of policy uncertainty. *Journal of Economic Dynamics and Control*, 59, 142–162.

Hommes, C. & Zhu, M. (2014). Behavioral learning equilibria. *Journal of Economic Theory*, 150, 778–814.

Hommes, C. H., Mavromatis, K., Ozden, T., & Zhu, M. (2019). Behavioral learning equilibria in the new keynesian model.

Ji, Y. & Xiao, W. (2016). Government spending multipliers and the zero lower bound. *Journal of Macroeconomics*, 48, 87–100.

Kim, C.-J. & Nelson, C. R. (1999). State-space models with regime switching: classical and gibbs-sampling approaches with applications. *MIT Press Books*, 1.

Kulish, M., Morley, J., & Robinson, T. (2017). Estimating dsge models with zero interest rate policy. *Journal of Monetary Economics*, 88, 35–49.

- Lansing, K. J. (2018). Endogenous regime switching near the zero lower bound.
- Lindé, J., Maih, J., & Wouters, R. (2017). *Estimation of Operational Macromodels at the Zero Lower Bound*. Technical report, Mimeo.
- Lindé, J., Smets, F., & Wouters, R. (2016). Challenges for central banks' macro models. In *Handbook of macroeconomics*, volume 2 (pp. 2185–2262). Elsevier.
- Liu, P. & Mumtaz, H. (2011). Evolving macroeconomic dynamics in a small open economy: An estimated markov switching dsge model for the uk. *Journal of Money, Credit and Banking*, 43(7), 1443–1474.
- Liu, Z., Waggoner, D. F., & Zha, T. (2011). Sources of macroeconomic fluctuations: A regime-switching dsge approach. *Quantitative Economics*, 2(2), 251–301.
- Maih, J. (2015). Efficient perturbation methods for solving regime-switching dsge models.
- Masolo, R. M. & Winant, P. E. (2019). The stochastic lower bound. *Economics Letters*, 180, 54–57.
- Milani, F. (2007). Expectations, learning and macroeconomic persistence. *Journal of monetary Economics*, 54(7), 2065–2082.
- Quaghebeur, E. (2018). Learning and the size of the government spending multiplier. *Macroeconomic Dynamics*, (pp. 1–36).
- Sims, C. A., Waggoner, D. F., & Zha, T. (2008). Methods for inference in large multiple-equation markov-switching models. *Journal of Econometrics*, 146(2), 255–274.
- Sims, C. A. & Zha, T. (2006). Were there regime switches in us monetary policy? *American Economic Review*, 96(1), 54–81.
- Slobodyan, S. & Wouters, R. (2012a). Learning in a medium-scale dsge model with expectations based on small forecasting models. *American Economic Journal: Macroeconomics*, 4(2), 65–101.
- Slobodyan, S. & Wouters, R. (2012b). Learning in an estimated medium-scale dsge model. *Journal of Economic Dynamics and control*, 36(1), 26–46.
- Smets, F. & Wouters, R. (2007). Shocks and frictions in us business cycles: A bayesian dsge approach. *American economic review*, 97(3), 586–606.
- Uhlig, H. F. et al. (1995). A toolkit for analyzing nonlinear dynamic stochastic models easily.

Woodford, M. (2013). Macroeconomic analysis without the rational expectations hypothesis. *Annu. Rev. Econ.*, 5(1), 303–346.

## Appendix

### A Long-run Taylor Principle

This section sketches the derivation of the Long-run Taylor Principle (LRTP) in Section 2.1. The readers are referred to Appendix A in [Davig & Leeper \(2007\)](#) for the full set of assumptions and the proof. LRTP refers to the determinacy of the Rational Expectations Equilibrium, which is defined as the existence of a unique bounded solution for the inflation process  $\pi_t$ . Recall that the process is given by:

$$\begin{bmatrix} \alpha_1 & 0 \\ 0 & \alpha_2 \end{bmatrix} \begin{bmatrix} \pi_{1,t} \\ \pi_{2,t} \end{bmatrix} = \begin{bmatrix} p_{11} & p_{12} \\ p_{21} & p_{22} \end{bmatrix} \begin{bmatrix} E_t \pi_{1,t+1} \\ E_t \pi_{2,t+1} \end{bmatrix} + \begin{bmatrix} r_t \\ r_t \end{bmatrix}. \quad (\text{A.1})$$

Define the matrix  $M = \begin{bmatrix} \alpha_1 & 0 \\ 0 & \alpha_2 \end{bmatrix}^{-1} \begin{bmatrix} p_{11} & p_{12} \\ p_{21} & p_{22} \end{bmatrix}$ . A necessary and sufficient condition for the determinacy of REE is that both eigenvalues of  $M$  lie inside the unit circle. The eigenvalues of  $M$  are given by:

$$\lambda_{1,2} = \frac{1}{2\alpha_1\alpha_2}(\alpha_2 p_{11} + \alpha_1 p_{22} \pm \sqrt{(\alpha_2 p_{11} - \alpha_1 p_{22})^2 + 4\alpha_1\alpha_2 p_{12}p_{21}}). \quad (\text{A.2})$$

[Davig & Leeper \(2007\)](#) show that, the condition:

$$(1 - \alpha_2)p_{11} + (1 - \alpha_1)p_{22} + \alpha_1\alpha_2 > 1, \quad (\text{A.3})$$

which is defined as the Long-run Taylor principle, is both necessary and sufficient for  $\lambda_{1,2}$  to lie inside the unit circle.

### B RPE and T-map

In this section we derive the T-map and the associated Restricted Perceptions Equilibria associated with the fixed point of the T-map for several cases.

## B.1 Special case with 2 regimes, no lagged variables

We first examine a special case with 2 regimes and no lagged state variables as presented in [2](#), where we can obtain an analytical expression for the RPE. Note that in the special case with  $\iota_p = 0$ , the solution to the model from Section [2.1](#) can be written as a generic 1-dimensional Markov-switching model of the form:

$$\begin{cases} \pi_t = d(s_t)r_t, \\ r_t = \rho r_{t-1} + v_t, \end{cases}$$

where  $d(s_t) = \frac{d\rho-1}{\alpha(s_t)}$ . The moments necessary for the T-map are given as follows:

$$E[\pi_t r_t] = P_1 E[\pi_t r_t | S_t = 1] + P_2 E[\pi_t r_t | S_t = 2],$$

$$\begin{aligned} E[\pi_t r_t | S_t = 1] &= E[d(s_t) r_t^2 | S_t = 1, S_{t-1} = 1] p_{11} + E[d(s_t) r_t^2 | S_t = 1, S_{t-1} = 2] (1 - p_{22}) \frac{P_2}{P_1} \\ &= d_1 p_{11} + d_1 (1 - p_{22}) \frac{P_2}{P_1}. \end{aligned}$$

Similarly, we have:

$$E[\pi_t r_t | S_t = 1] = d_2 p_{22} + d_2 (1 - p_{11}) \frac{P_1}{P_2},$$

which yields:

$$E[\pi_t r_t] = P_1 (d_1 p_{11} + d_1 (1 - p_{22}) \frac{P_2}{P_1}) + P_2 (d_2 p_{22} + d_2 (1 - p_{11}) \frac{P_1}{P_2}).$$

Plugging in the steady-state probabilities  $P_1$  and  $P_2$ , the T-map is given as follows:

$$d \rightarrow T(d) = \frac{\alpha_1(1 - p_{22}) + \alpha_2(1 - p_{11})}{\alpha_1 \alpha_2 (2 - p_{11} - p_{22})} (d\rho + 1),$$

with the E-stability condition:

$$DT_a = \frac{\alpha_1(1 - p_{22}) + \alpha_2(1 - p_{11})}{\alpha_1 \alpha_2 (2 - p_{11} - p_{22})} \rho < 1.$$

Re-arranging the expression above yields the Long-run E-stability (LRES) condition presented in Section [2](#). Further note that the regime-specific T-maps, and the associated regime-specific E-stability conditions are given by:

$$d \rightarrow \frac{d\rho + 1}{\alpha_i},$$

$$DT_d = \frac{\rho}{\alpha_i} < 1,$$

which implies that E-stability of all regime-specific equilibria is a sufficient, but not necessary condition for LRES.

## B.2 1-dimensional case with m regimes

We next generalize the T-map and RPE to the generic case with lagged state variables and m regimes. While the T-map becomes analytically intractable in this case, we can still numerically compute it in the 1-dimensional case. Note that the Fisherian model considered in Section 2.2 can be written as a generic 1-dimensional Markov-switching model of the form:

$$\begin{cases} \pi_t = d(s_t)r_t + b(s_t)\pi_{t-1}, \\ r_t = \rho r_{t-1} + v_t, \end{cases}$$

where  $b(s_t) = \frac{\iota_p}{\alpha(s_t) - (1-\iota_p)b}$  and  $d(s_t) = \frac{(1-\iota_p)d\rho+1}{\alpha(s_t) - (1-\iota_p)b}$ . In this Section we consider the general case with  $m$  regimes, with transition matrix given by:

$$Q = \begin{bmatrix} p_{11} & \dots & p_{1m} \\ \vdots & \dots & \vdots \\ p_{m1} & \dots & p_{mm} \end{bmatrix}.$$

The 2-regime setup of Section 2.2 is a special case with  $m = 2$ . We omit the first moment  $E[\pi_t]$ , which is trivially given as zero. Using this, we compute the second moments starting with the conditional variance. We have:

$$E[\pi_t^2] = \sum_{i=1}^m P_i E[\pi_t^2 | S_t = i],$$

$$E[\pi_t^2 | S_t = i] \sum_{j=1}^m E[\pi_t^2 | S_t = i, S_{t-1} = j] p_{ji} \frac{P_j}{P_i},$$

where  $P_i$  denotes the  $i^{th}$  element of the steady-state vector of the Markov chain. Plugging in the expression for  $\pi_t$  yields:

$$\begin{aligned} &= \sum_{j=1}^m E[d(s_t)^2 r_t^2 + b(s_t)^2 \pi_{t-1}^2 + 2b(s_t)d(s_t)r_t\pi_{t-1} | S_t = i, S_{t-1} = j] p_{ji} \frac{P_j}{P_i} \\ &= \sum_{j=1}^m E[d_i^2 \sigma_r^2 + b_i^2 \pi_{t-1}^2 + \sigma_r^2 + 2b_1 d_i r_t \pi_{t-1} | S_{t-1} = j] p_{ji} \frac{P_j}{P_i}. \end{aligned}$$

Note that this last expression implies  $m$  equations in  $m$  unknowns for the conditional variances, given the conditional covariances  $E[\pi_t r_t | S_t = j]$ . Using this, the unconditional variance is given by:

$$E[\pi_t^2] = \sum_{i=1}^m P_i \sum_{j=1}^m (d_i^2 \sigma_r^2 + b_i^2 E[\pi_{t-1}^2 | S_t = j] + \sigma_r^2 + 2b_i d_i r_t E[\pi_{t-1} | S_{t-1} = j]) p_{ji} \frac{P_j}{P_i}.$$

Next we move onto the covariance term  $E[\pi_t r_t]$ :

$$\begin{aligned} E[\pi_t r_t] &= \sum_{i=1}^m P_i E[\pi_t r_t | S_t = i], \\ E[\pi_t r_t | S_t = i] &= \sum_{j=1}^m E[\pi_t r_t | S_t = i, S_{t-1} = j] p_{ji} \frac{P_j}{P_i} \\ &= \sum_{j=1}^m E[b(s_t) \pi_{t-1} r_t + d(s_t) r_t^2 | S_t = i, S_{t-1} = j] p_{ji} \frac{P_j}{P_i} \\ &\quad \sum_{i=1}^m (b_i \rho E[\pi_t r_t | S_t = j] + d_i \sigma_r^2) p_{ji} \frac{P_j}{P_i}. \end{aligned}$$

Note that again, the last expression implies  $m$  equations in  $m$  unknowns for the conditional covariances. With this, the unconditional covariance is given by:

$$E[\pi_t r_t] = \sum_{i=1}^m m P_i \sum_{j=1}^m (b_i \rho E[\pi_t r_t | S_t = j] + d_i \sigma_r^2) p_{ji} \frac{P_j}{P_i}.$$

Next we compute the first-order autocovariance:

$$\begin{aligned} E[\pi_t \pi_{t-1}] &= \sum_{i=1}^m P_i E[\pi_t \pi_{t-1} | S_t = i], \\ E[\pi_t \pi_{t-1} | S_t = i] &= \sum_{j=1}^m E[b(s_t) \pi_{t-1}^2 + d(s_t) \pi_{t-1} r_t | S_t = i, S_{t-1} = j] p_{ji} \frac{P_j}{P_i} \\ &= \sum_{j=1}^m (b_i E[\pi_t^2 | S_t = j] + d_i \rho E[\pi_t r_t | S_t = j]) p_{ji} \frac{P_j}{P_i}. \end{aligned}$$

Given the conditional covariance and conditional variance terms, the above expression yields the conditional autocovariances. Hence the unconditional autocovariance is given as:

$$E[\pi_t \pi_{t-1}] = \sum_{i=1}^m P_i \sum_{j=1}^m (b_i E[\pi_t^2 | S_t = j] + d_i \rho E[\pi_t r_t | S_t = j]) p_{ji} \frac{P_j}{P_i}.$$

Finally note that:

$$E[d(s_t)\pi_{t-1}r_t] = \sum_{i=1}^m P_i \sum_{j=1}^m d_i \rho E[\pi_t r_t | S_t = j] p_{ji} \frac{P_j}{P_i},$$

and:

$$E[b(s_t)\pi_{t-1}r_t] = \sum_{i=1}^m P_i \sum_{j=1}^m b_i \rho E[\pi_t r_t | S_t = j] p_{ji} \frac{P_j}{P_i}.$$

Recalling the T-map  $\begin{pmatrix} d \\ b \end{pmatrix} \rightarrow T(d, b) = \begin{pmatrix} E[(\pi_t - b\pi_{t-1})r_t] \\ \frac{E[(\pi_t - dr_t)\pi_{t-1}]}{E[\pi_t^2]} \end{pmatrix}$ , the above conditions fully pin down  $T(d, b)$ . It is generally not possible to obtain analytical expressions for this mapping, which also applies to the RPE values  $d^{RPE}$  and  $b^{RPE}$ . Therefore our results in Section 2.2 are computed numerically for given values of parameters.

### B.3 N dimensional case with m regimes

In this section we derive the T-map for the general N dimensional case with m regimes. After plugging in the PLM into ALM, the model can be re-written as a generic Markov-switching model of the form:

$$\begin{cases} X_t = a(s_t) + b(s_t)X_{t-1} + d(s_t)\epsilon_t, \\ \epsilon_t = \rho\epsilon_{t-1} + \eta_t, \end{cases}$$

where  $a(s_t) = (I - C(s_t)b)^{-1}(A(s_t) + C(s_t)a)$ ,  $b(s_t) = (I - C(s_t)b)^{-1}B(s_t)$  and  $d(s_t) = (I - C(s_t)b)^{-1}(C(s_t)(d\rho) + D(s_t))$ . We need the first and second moments of this system in order to compute the resulting T-map for the RPE. Starting with the first moment, we have:

$$\begin{aligned} E[X_t] &= \sum_{i=1}^m P_i E[X_t | S_t = i], \\ E[X_t | S_t = i] &= \sum_{j=1}^m [a_i + b_i X_{t-1} + d_i \epsilon_t | S_{t-1} = j] p_{ji} \frac{P_j}{P_i} \\ &= \sum_{j=1}^m (a_i + b_i E[X_t | S_t = j]) p_{ji} \frac{P_j}{P_i}. \end{aligned}$$

The expression above implies m equations in m unknowns for the conditions means. Using this yields:

$$E[X_t] = \sum_{i=1}^m P_i \sum_{j=1}^m (a_i + b_i E[X_t | S_t = j]) p_{ji} \frac{P_j}{P_i}.$$

Moving onto the second moments and starting with the covariance term, we have:

$$E[X_t \epsilon'_t] = \sum_{i=1}^m P_i E[X_t \epsilon'_t | S_t = i],$$

$$\begin{aligned} & E[X_t \epsilon'_t | S_t = i] E[()a(s_t) + b(s_t)X_{t-1} + d(s_t)\epsilon_t) \epsilon'_t | S_t = i] \\ &= \sum_{j=1}^m E[(a_i + b_i X_{t-1} + d_i \epsilon_t) \epsilon'_t | S_{t-1} = j] p_{ji} \frac{P_j}{P_i} \\ &= \sum_{j=1}^m (b_i \rho E[X_t \epsilon'_t | S_t = j] + d_i \Sigma_\epsilon) p_{ji} \frac{P_j}{P_i}. \end{aligned}$$

The last expression again implies  $m$  equations in  $m$  unknowns for the conditional covariances. The unconditional covariance is then given by:

$$E[X_t \epsilon'_t] = \sum_{i=1}^m P_i \sum_{j=1}^m (b_i \rho E[X_t \epsilon'_t | S_t = j] + d_i \Sigma_\epsilon) p_{ji} \frac{P_j}{P_i}.$$

Next we compute:

$$\begin{aligned} E[X_t X'_t] &= \sum_{i=1}^m P_i E[X_t X'_t | S_t = i], \\ E[X_t X'_t | S_t = i] &= E[a(s_t)a(s_t)' + 2a(s_t)X'_{t-1}b(s_t)' + 2a(s_t)\epsilon_t d(s_t)' + \\ &\quad b(s_t)X_{t-1}X'_{t-1}b(s_t)' + 2b(s_t)X_{t-1}\epsilon_t d(s_t)' + d(s_t)\epsilon_t \epsilon'_t d(s_t)' | S_t = i] \\ &= \sum_{j=1}^m E[a_i a'_i 2a_i X'_{t-1} b'_i + 2a_i \epsilon'_t d'_i + b_i X_{t-1} X'_{t-1} b'_i + 2b_i X_{t-1} \epsilon'_t d'_i + d_i \epsilon_t \epsilon'_t d'_i | S_t = j] p_{ji} \frac{P_j}{P_i}. \end{aligned}$$

Given the conditional means and covariances, the last expressions implies  $m$  equations in  $m$  unknowns for the conditional moments  $E[X_t X'_t | S_t = i]$ . The unconditional moment is then given by:

$$E[X_t X'_t] = \sum_{i=1}^m P_i \sum_{j=1}^m (a_i a'_i + 2a_i E[X'_t | S_t = j] b'_i + b_i E[X_t X'_t | S_t = j] b'_i + 2b_i E[X_t \epsilon'_t | S_t = j] \rho' d'_i + d_i \Sigma_\epsilon d'_i) p_{ji} \frac{P_j}{P_i}.$$

Finally we compute the autocovariance term:

$$E[X_t X'_{t-1}] = \sum_{i=1}^m P_i E[X_t X'_{t-1} | S_t = i],$$

$$E[X_t X'_{t-1} | S_t = i] = E[a_i X'_{t-1} + b_i X_{t-1} X'_{t-1} + d_i \rho \epsilon_{t-1} X'_{t-1} | S_t = i] =$$

$$\sum_{j=1}^m (a_i E[X_t | S_t = j] + b_i E[X_t X'_t | S_t = j] + d_i \rho E[\epsilon_t X'_t | S_t = j]) p_{ji} \frac{P_j}{P_i}.$$

The last expression is pinned by the conditional first and second moments computed above. The unconditional autocovariance is then given as:

$$E[X_t X'_t] = \sum_{i=1}^m \sum_{j=1}^m (a_i E[X_t | S_t = j] + b_i E[X_t X'_t | S_t = j] + d_i \rho E[\epsilon_t X'_t | S_t = j]) p_{ji} \frac{P_j}{P_i}.$$

Recall that the T-map is given by:

$$\begin{pmatrix} a \\ b \\ c \end{pmatrix} \rightarrow \begin{pmatrix} E[X_t - bX_{t-1} - d\epsilon_t] \\ E[(X_t - a - d\epsilon_t)X'_{t-1}]E[X_t X'_t]^{-1} \\ E[(X_t - a - bX_{t-1})\epsilon'_t]E[\epsilon_t \epsilon'_t]^{-1} \end{pmatrix}.$$

Hence, given the first and second moments computed above, the T-maps for  $a$ ,  $b$  and  $c$  are pinned down. Similar to 1-dimensional case, it is generally not possible to find analytical expressions for these matrices. Further note that, the T-map for  $b \rightarrow T(a, b, c)$  involves a  $2^{th}$  order matrix polynomial of dimension  $N$ . This means there can be up to  $\binom{2N}{N}$  for  $b$ . To our knowledge, there is no straightforward and general method to compute the full set of solutions to this problem. In this paper, we do not compute these fixed-points and rely on Monte Carlo simulations when necessary.

Further note that the regime-specific T-maps are given by:

$$\begin{pmatrix} a \\ b \\ c \end{pmatrix} \rightarrow \begin{pmatrix} A_i + C_i(a + ba) \\ B_i + C_i b^2 \\ C_i(bd + d\rho) + D_i \end{pmatrix}.$$

These simply correspond to the standard MSV solutions given the regime-specific matrices. Computing the fixed-points yield the regime-specific equilibria as follows:

$$\begin{cases} a^{R_i} = (I - C_i - C_i b^{R_i})^{-1} A_i, \\ vec(D^{R_i}) = (I - (I \otimes (C_i b^{R_i}))) vec(d) + (\rho \otimes C_i) vec(d) + vec(D_i), \end{cases}$$

which yields the regime-specific values for  $a^{R_i}$  and  $d^{R_i}$  respectively, for a given matrix  $b^{R_i}$ . The second-order polynomial for  $b^{R_i}$  can be solved using standard toolboxes such as [Adjemian et al. \(2011\)](#) and [Uhlig et al. \(1995\)](#), which then completely pins down the regime-specific MSV. Denoting  $\theta = (a, b, d)'$ , the associated Jacobian for E-stability condition is given by:

$$\frac{DT}{D\theta} = \begin{bmatrix} C_i + C_i b & \text{vec}_{n,n}^{-1}(a' \otimes C_i) & 0 \\ 0 & 2C_i b & 0 \\ 0 & \text{vec}_{n,n}^{-1}(d' \otimes C_i) & C_i b + \text{vec}_{n,n}^{-1}(\rho' \otimes C_i) \end{bmatrix},$$

where  $\text{vec}_{n,n}^{-1}$  denotes the matricization of a vector to an  $(n, n)$  matrix.

## B.4 Long-run E-stability for the New Keynesian Model

This section derives the long-run E-stability conditions for an extended version of the New Keynesian model from Section 2. The main purpose is to investigate how the presence of exogenous shocks affects the stability conditions presented in Section 2. Consider the following version of the New Keynesian model with two exogenous AR(1) shocks:

$$\begin{cases} x_t = E_t x_{t+1} - \frac{1}{\tau}(r_t - E_t \pi_{t+1}) + \epsilon_{x,t}, \\ \pi_t = \beta E_t \pi_{t+1} + \kappa x_t + \epsilon_{\pi,t}, \\ r_t = \max\{0, \phi_x x_t + \phi_\pi \pi_t + \eta_{r,t}\}, \\ \epsilon_{x,t} = \rho_x \epsilon_{x,t-1} + \eta_{x,t}, \\ \epsilon_{\pi,t} = \rho_\pi \epsilon_{\pi,t-1} + \eta_{\pi,t}, \end{cases}$$

We first derive the regime-specific T-maps and the associated Jacobian matrix. Using the same notation from Section B.3, we have:

$$\begin{pmatrix} a \\ d \end{pmatrix} \rightarrow T(a, d) = \begin{pmatrix} A_i + C_i a \\ C_i d \rho + D_i \end{pmatrix}, \quad \frac{\partial T(a, d)}{\partial [a, d]} = \begin{pmatrix} C_i & 0 \\ 0 & (\rho C_i)' \end{pmatrix},$$

where the underlying Rational Expectations Equilibrium is given by  $a = (I - C_i)^{-1} A_i$  (which reduces to a vector of zeros in this example) and  $\text{vec}(d) = (I - \rho' \otimes C_i)^{-1} \text{vec}(D_i)$ . Notice first that, given the Jacobian matrix as above, the first part on the diagonal governs the stability of mean dynamics  $a$ , while the second part governs the stability of shock coefficients  $d$ . As such, the underlying E-stability conditions for the means and shocks are independent. Second, with shock autocorrelation values of  $0 < \rho_x < 1$  and  $0 < \rho_\pi < 1$ , the eigenvalues associated with the stability of  $d$  are always smaller than the eigenvalues of  $a$ . Therefore, the E-stability condition on the mean dynamics acts as a sufficient condition for E-stability on the shock dynamics. For the parameterization that we considered in Section 2, autocorrelation parameters with values  $\rho_x < 0.87$  and  $\rho_\pi < 0.87$  guarantee that the shock dynamics around  $d$  are E-stable in both normal and ELB regimes. Therefore the stability conditions considered in Section 2 fully

extend to this case with exogenous shocks, without loss of generality.

For completeness, we also provide the RPE and the associated long-run E-stability for the model. For the T-map, we obtain:

$$\begin{pmatrix} a \\ d \end{pmatrix} \rightarrow T(a, d) = \begin{pmatrix} P_1(A_1 + C_1 a) + P_2(A_2 + C_2 a) \\ P_1(C_2 d\rho + D_2) + P_2(C_2 d\rho + D_2) \end{pmatrix}, \frac{\partial T(a, d)}{\partial [a, d]} = \begin{pmatrix} P_1 C_1 + P_2 C_2 & 0 \\ 0 & P_1(\rho C_1)' + P_2(\rho C_2)' \end{pmatrix},$$

where the RPE is given by:

$$\begin{cases} a = (I - P_1 C_1 - P_2 C_2)^{-1}(P_1 A_1 + P_2 A_2), \\ d = (I - \rho' \otimes (P_1 C_1) - \rho' \otimes (P_2 C_2))^{-1}(\text{vec}(P_1 D_1) + \text{vec}(P_2 D_2)). \end{cases}$$

Hence, in the absence of lagged variables, the equilibrium and the associated stability conditions still come out simply as weighted averages of the underlying regime-specific equilibria.

## C Kim-Nelson Filter

This section provides a more detailed description of the KN-filter used in our estimations. The filter nests the standard Kalman filter for unobserved state variables with the Hamilton filter for unobserved regime probabilities. These two filters are followed by an approximation step via collapsing, which reduces the number of states from  $m^2$  to  $m$  in order to keep the algorithm tractable. We extend the filter with an adaptive learning step, which takes a weighted average of the (Kalman) filtered states based on the (Hamilton) filtered regime probabilities. We assume that the resulting states are observable to the model's agents, who update their beliefs with a constant gain least squares algorithm using the latest available data. This leaves the Kalman and Hamilton filter blocks intact, since the model is conditionally linear at every period, given the previous period's adaptive learning update.

The endogenous regime-switching model follows from a simple extension of the above filter, where the transition probability matrix  $Q(i, j)$  with a time-varying matrix  $Q_t(i, j)$ . This matrix is updated every period after the Kalman filter block given the shadow rate, which in turn is calculated based on the inflation and output gap variables contained in matrices  $S_{t|t}^{(i,j)}$ .

Table 7: KN-filter for Markov-Switching DSGE Models under Adaptive Learning

$$\begin{cases} S_t = \gamma_{2,\Phi_t}^{(s_t)} + \gamma_{1,\Phi_t}^{(s_t)} S_{t-1} + \gamma_{3,\Phi_t}^{(s_t)} \epsilon_t, \\ y_t = E + F S_t \end{cases}, \epsilon_t \sim N(0, \Sigma)$$

0) Initial States:

$$\tilde{S}_{0|0}^i, \tilde{P}_{0|0}^i, Pr[S_0 = i|\Phi_0], \Phi_0 \text{ given.}$$

1) Kalman Filter Block with the standard measurement and transition equations:

For  $t = 1 : N$   
For  $\{S_{t-1} = i, S_t = j\}$

$$\begin{cases} S_{t|t-1}^{(i,j)} = \gamma_1^{(j)} S_{t-1|t-1}^{(i)} + \gamma_2^{(j)} \\ P_{t|t-1}^{(i,j)} = \gamma_1^{(j)} P_{t-1|t-1}^{(i)} \gamma_1^{(j)} + \gamma_3^{(j)} \Sigma^{(j)} (\gamma_3^{(j)})' \\ v_{t|t-1}^{(i,j)} = (y_t - F^{(j)} S_{t|t-1}^{(i,j)}) \\ F e^{(i,j)} = F^{(j)} P_{t|t-1}^{(i,j)} F^{(j)} \\ S_{t|t}^{(i,j)} = S_{t|t-1}^{(i,j)} + P_{t|t-1}^{(i,j)} (F^{(j)})' (F e^{(i,j)})^{-1} v^{(i,j)} \\ P_{t|t}^{(i,j)} = P_{t|t-1}^{(i,j)} (F^{(j)})' (F e^{(i,j)})^{-1} F^{(j)} P_{t|t-1}^{(i,j)} \end{cases}$$

2) Hamilton Block for transition probabilities:

Denote:  $Pr[S_{t-1} = i, S_t = j|\Phi_{t-1}] = pp_{t|t-1}^{i,j} f(y_t|\Phi_{t-1})$  the marginal likelihood,

$Pr[S_{t-1} = i, S_t = j|\Phi_t] = pp_{t|t}^{i,j}$  and  $Pr[S_t = j|\Phi_t] = pp_{t|t}^{j\tilde{j}}$

$$\begin{cases} pp_{t|t-1}^{(i,j)} = Q(i,j) pp_{t-1|t-1}^{(i)} \\ f(y_t|\Phi_{t-1}) = \sum_{j=1}^M \sum_{i=1}^M f(y_t|S_{t-1} = i, S_t = j, \Phi_{t-1}) pp_{t|t-1}^{(i,j)} \\ pp_{t|t}^{(i,j)} = \frac{f(y_t|S_{t-1} = i, S_t = j, \Phi_{t-1}) pp_{t|t-1}^{(i,j)}}{f(y_t|\Phi_{t-1})} \\ p_{t|t}^j = \sum_i^M pp_{t|t}^{(i,j)} \end{cases}$$

3) Collapsing to reduce the number of states from  $m^2$  to m:

$$\begin{cases} S_{t|t}^{(i)} = \frac{\sum_{j=1}^M pp_{t|t}^{(i,j)} S_{t|t}^{(i,j)}}{p_{t|t}^{(j)}} \\ P_{t|t}^{(i)} = \frac{\sum_{j=1}^M pp_{t|t}^{(i,j)} (P_{t|t}^{(i,j)} + (S_{t|t}^{(j)} - S_{t|t}^{(i,j)}) (S_{t|t}^{(j)} - S_{t|t}^{(i,j)})')} {p_{t|t}^{(j)}} \end{cases}$$

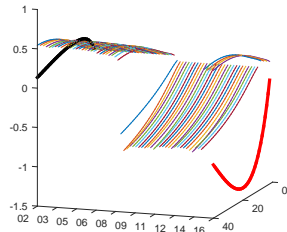
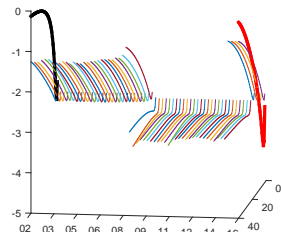
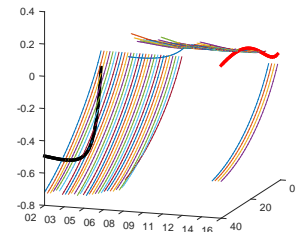
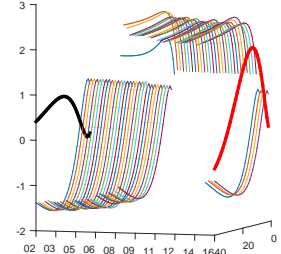
4) Update expectations based on filtered states:

Updating Expectations based on Filtered States:

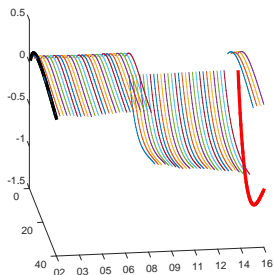
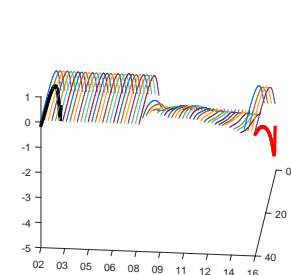
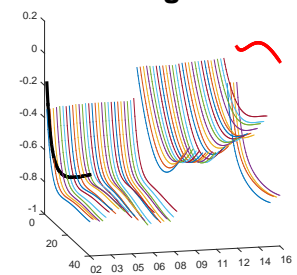
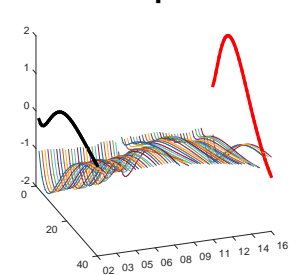
$$\begin{cases} \tilde{S}_{t|t} = \sum_{j=1}^M p_{t|t}^{(j)} S_{t|t}^{(j)} \\ \Phi_t = \Phi_{t-1} + \gamma R_t^{-1} \tilde{S}_{t-1|t-1} (\tilde{S}_{t|t} - \Phi_{t-1}^T \tilde{S}_{t-1|t-1})^T \\ R_t^{-1} = R_{t-1} + \gamma (\tilde{S}_{t-1|t-1} \tilde{S}_{t-1|t-1}^T - R_{t-1}) \end{cases}$$

## D Additional Impulse Responses

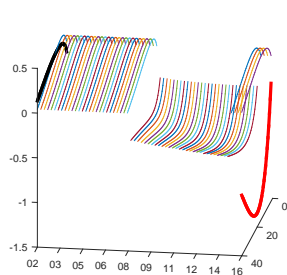
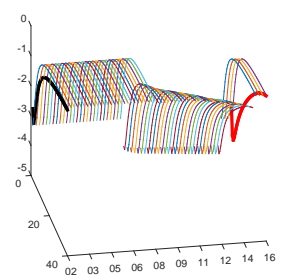
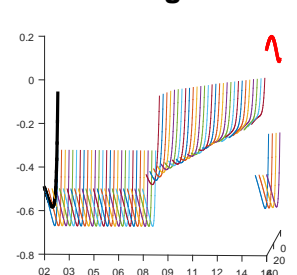
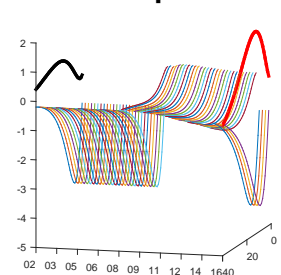
This section provides the time-varying impulse responses for investment and consumption in Figures 14 and 15. As already discussed in Section 4, the IRFs are characterized by two jumps in 2008 and 2015, with the entry to and exit from the ELB regime. For the AR(1) model, the overall time variation for all shocks is fairly small compared to the jump in 2008. For the LIL and MSV models, and particularly for the productivity and government spending shocks, we observe a gradual movement in the direction of the REE-MS impulse responses.

$\eta_a$  $\eta_b$  $\eta_g$  $\eta_p$ 

(a) AR(1)

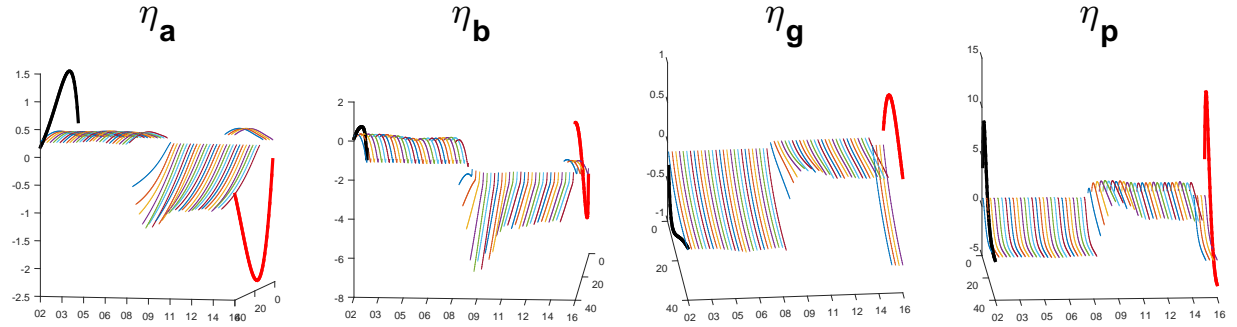
 $\eta_a$  $\eta_b$  $\eta_g$  $\eta_p$ 

(b) LIL

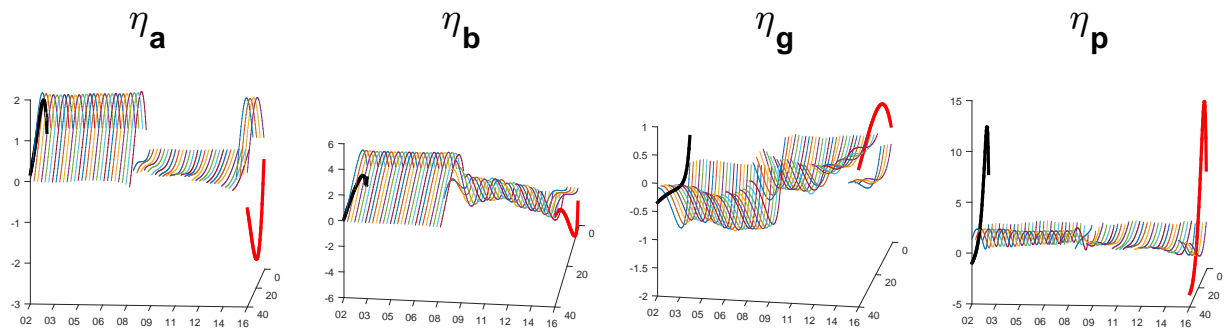
 $\eta_a$  $\eta_b$  $\eta_g$  $\eta_p$ 

(c) MSV

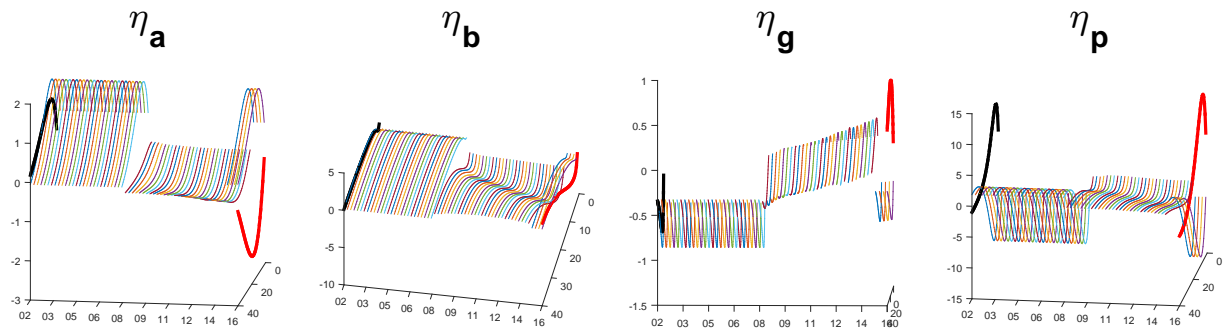
**Figure 14: Consumption:** Comparison of learning IRFs with REE IRFs. Each IRF shows a one standard deviation shock of  $\eta_a, \eta_b, \eta_g, \eta_p$  respectively.



(a) AR(1)



(b) LIL



(c) MSV

Figure 15: **Investment:** Comparison of learning IRFs with REE IRFs. Each IRF shows a one standard deviation shock of  $\eta_a, \eta_b, \eta_g, \eta_p$  respectively.

## E Smets-Wouters Model Description

The model consists of 13 equations linearized around the steady-state growth path, supplemented with seven exogenous structural shocks. We have two minor deviations from the benchmark model. First, we assume that the mark-up shocks follow AR(1) processes, as opposed to ARMA(1,1) processes assumed in the original model. Second, we define output gap as the deviation of output from the underlying productivity process following [Slobodyan & Wouters \(2012a\)](#), as opposed to the original model that defines output gap based on the flexible economy. This second deviation allows us to restrict the state-space of the model by omitting the flexible part of the economy, thereby reducing the computational costs. The rest of the model follows the same structure as the original model. The readers are referred to [Smets & Wouters \(2007\)](#) for further details about the microfoundations. In this section, we briefly outline the linearized model used in our estimations.

The aggregate resource constraint is given by:

$$\begin{cases} y_t = c_y c_t + i_y i_t + z_y z_t + \epsilon_t^g, \\ \epsilon_t^g = \rho_g \epsilon_{t-1}^g + \eta_t^g, \end{cases} \quad (\text{E.1})$$

where  $y_t$ ,  $c_t$ ,  $i_t$  and  $z_t$  are the output, consumption, investment and capital utilization rate respectively, while  $c_y$ ,  $i_y$  and  $z_y$  are the steady-state shares in output of the respective variables. The second equation defines the exogenous spending shock  $\epsilon_t^g$  where  $\eta_t^g$  is an i.i.d-normal disturbance for spending. The consumption Euler equation is given by:

$$\begin{cases} c_t = c_1 c_{t-1} + (1 - c_1) \mathbb{E}_t c_{t+1} + c_2 (l_t - \mathbb{E}_t l_{t+1}) - c_3 (r_t - \mathbb{E}_t \pi_{t+1}) + \epsilon_t^b, \\ \epsilon_t^b = \rho_b \epsilon_{t-1}^b + \eta_t^b, \end{cases} \quad (\text{E.2})$$

with  $c_1 = \frac{\lambda}{\gamma}(1 + \frac{\lambda}{\gamma})$ ,  $c_2 = (\sigma_c - 1)(w_{ss} l_{ss}/c_{ss})/(\sigma_c(1 + \frac{\lambda}{\gamma})$ ,  $c_3 = (1 - \frac{\lambda}{\gamma})/((1 + \frac{\lambda}{\gamma})\sigma_c)$ , where  $\lambda$ ,  $\gamma$  and  $\sigma_c$  denote the habit formation in consumption, steady state-growth rate and the elasticity of intertemporal substitution respectively.  $\epsilon_t^b$  corresponds to the risk premium shock modeled as an AR(1) process, where  $\eta_t^b$  is an i.i.d-normal disturbance. Next, the investment Euler equation is defined as:

$$\begin{cases} i_t = i_1 i_{t-1} + (1 - i_1) \mathbb{E}_t i_{t+1} + i_2 q_t + \epsilon_t^i, \\ \epsilon_t^i = \rho_i \epsilon_{t-1}^i + \eta_t^i, \end{cases} \quad (\text{E.3})$$

with  $i_1 = \frac{1}{1 + \bar{\beta}\gamma}$ ,  $i_2 = \frac{1}{(1 + \bar{\beta}\gamma)(\gamma^2 \phi)}$ , where  $\bar{\beta} = \beta \gamma^{-\sigma_c}$ ,  $\phi$  is the steady-state elasticity of capital adjustment cost and  $\beta$  is the HH discount factor.  $q_t$  denotes the real value of existing capital stock.  $\epsilon_t^i$  represents the AR(1) investment shock , where  $\eta_t^i$  is an i.i.d-normal disturbance. The

value of capital-arbitrage equation is given by:

$$q_t = q_1 \mathbb{E}_t q_{t+1} + (1 - q_1) \mathbb{E}_t r_{t+1}^k - (r_t + \mathbb{E}_t \pi_{t+1}) + \frac{1}{c_3} \epsilon_t^b, \quad (\text{E.4})$$

with  $q_1 = \bar{\beta}(1 - \delta)$ . The production function is given as:

$$\begin{cases} y_t = \phi_p(\alpha k_t^s + (1 - \alpha)l_t + \epsilon_t^a), \\ \epsilon_t^a = \rho_a \epsilon_{t-1}^a + \eta_t^a, \end{cases} \quad (\text{E.5})$$

where  $k_t^s$  denotes the capital services used in production,  $\alpha$  is the share of capital in production and  $\phi_p$  is ( one plus) the share of fixed costs in production.  $\epsilon_t^a$  denotes the AR(1) total factor productivity shock. Capital is assumed to be the sum of the previous amount of capital services used and the degree of capital utilization, hence:

$$k_t^s = k_{t-1} + z_t. \quad (\text{E.6})$$

The degree of capital utilization is a positive function of the degree of rental rate,  $z_t = z_1 r_t^k$ , with  $z_1 = \frac{1-\psi}{\psi}$ ,  $\psi$  the elasticity of the capital utilization adjustment cost. Next the equation for installed capital is given by:

$$k_t = k_1 k_{t-1} + (1 - k_1) i_t + k_2 \epsilon_t^i, \quad (\text{E.7})$$

with  $k_1 = \frac{1-\delta}{\gamma}$ ,  $k_2 = (1 - \frac{1-\delta}{\gamma})(1 + \bar{\beta}\gamma)\gamma^2\phi$ . The price mark-up equation is given by:

$$\mu_t^p = \alpha(k_t^s - l_t) + \epsilon_t^a - w_t. \quad (\text{E.8})$$

The NKPC is characterized as:

$$\begin{cases} \pi_t = \pi_1 \mathbb{E}_t \pi_{t+1} - \pi_2 \mu_t^p + \epsilon_t^p, \\ \epsilon_t^p = \rho_p \epsilon_{t-1}^p + \eta_t^p, \end{cases} \quad (\text{E.9})$$

with  $\pi_1 = \bar{\beta}\gamma$ ,  $\pi_2 = (1 - \beta\gamma\xi_p)(1 - \xi_p)/[\xi_p((\phi_p - 1)\epsilon_p + 1)]$ , where  $\xi_p$  corresponds to the degree of price stickiness, while  $\epsilon_p$  denotes the Kimball goods market aggregator. The rental rate of capital is given by:

$$r_t^k = -(k_t - l_t) + w_t, \quad (\text{E.10})$$

The wage mark-up is given as the real wages net of marginal rate of substitution between

working and consuming, hence:

$$\mu_t^w = w_t - (\sigma_l l_t + \frac{1}{1 - \lambda/\gamma} (c_t - \frac{\lambda}{\gamma} c_{t-1})), \quad (\text{E.11})$$

where  $\sigma_l$  denotes the elasticity of labor supply. The real wage equation is given by:

$$\begin{cases} w_t = w_1 w_{t-1} + (1 - w_1) (\mathbb{E}_t w_{t+1} + \mathbb{E}_t \pi_{t+1}) - w_2 \mu_t^w + \epsilon_t^w, \\ \epsilon_t^w = \rho_w \epsilon_{t-1}^w + \eta_t^w, \end{cases} \quad (\text{E.12})$$

with  $w_1 = 1/(1 + \bar{\beta}\gamma)$ , and  $w_2 = ((1 - \bar{\beta}\gamma\xi_w)(1 - \xi_w)/(\xi_w(\phi_w - 1)\epsilon_w + 1))$ . Hence the real wage is a weighted average of the past and expected wage, expected inflation, the wage mark-up and the wage mark-up shock  $\epsilon_t^w$ , where  $\eta_t^w$  is an i.i.d-normal disturbance. Finally, monetary policy is assumed to follow a standard Taylor rule subject to the ELB constraint:<sup>40</sup>

$$\begin{cases} r_t = \max\{-\bar{r}, \rho r_{t-1} + (1 - \rho)(r_\pi \pi_t + r_y x_y) + r_{dy}(\Delta x_t) + \epsilon_t^r\}, \\ \epsilon_t^r = \rho_r \epsilon_{t-1}^r + \eta_t^r, \end{cases} \quad (\text{E.13})$$

where  $\bar{r}$  denotes the steady-state interest rate,  $x_t$  denotes the output gap, and  $\epsilon_t^r$  is the AR(1) monetary policy shock. As explained in Section 4, this is approximated as a 2-regime Markov-process, where:

$$r_t = \rho(s_t)r_{t-1} + (1 - \rho(s_t))(r_\pi(s_t)\pi_t + r_y(s_t)x_y) + r_{dy}(s_t)(\Delta x_t) + \epsilon_t^r(s_t), \quad (\text{E.14})$$

with the normal regime given as  $\rho(s_t = 1) > 0$ ,  $r_\pi(s_t = 1) > 1$ ,  $r_y(s_t = 1) > 0$ ,  $r_{dy}(s_t = 1) > 0$  and  $\epsilon_t^r(s_t = 1)$  an AR(1) process with persistence  $\rho_r$ , where the i.i.d. disturbances have a standard deviation of  $\eta_{r_N}$ . The ELB regime is given as a pegged interest rate rule with  $\rho(s_t = 2) = 0$ ,  $r_\pi(s_t = 2) = 0$ ,  $r_y(s_t = 2) = 0$ ,  $r_{dy}(s_t = 2) = 0$  and  $\epsilon_t^r(s_t = 2)$  a white noise process with standard deviation  $\eta_{r_{ELB}}$ . In this paper, following the approach in Slobodyan & Wouters (2012a), we deviate from the original Smets-Wouters model and define the output gap as the deviation of output from the underlying productivity process, i.e.  $x_t = y_t - \epsilon_t^a$ . This reduces the number of forward-looking variables from 12 to 7, thereby reducing the computational costs of estimating the model.

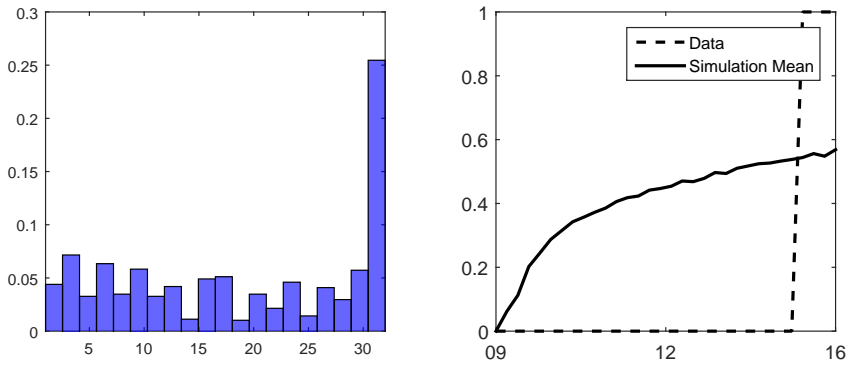
---

<sup>40</sup>Note that in Sections 2 through 4, we denote the nominal interest rate by  $i_t$ . In this Appendix, with some abuse of notation, we use  $i_t$  to denote investment, whereas the nominal interest rate is denoted by  $r_t$ .

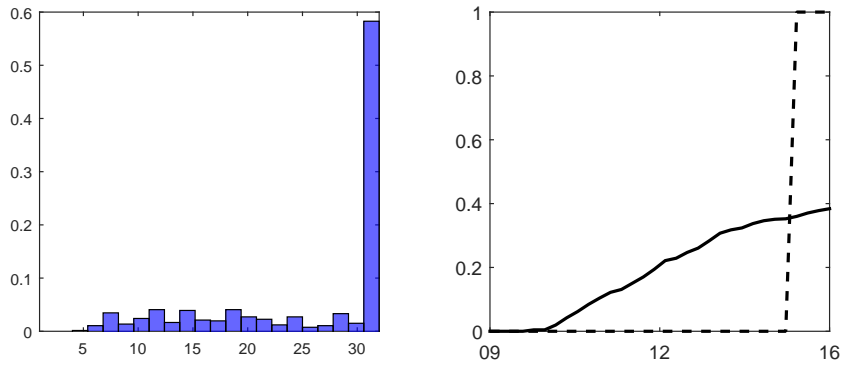
## F Additional Figures from Counterfactual Simulations

This section provides some complementary results for the counterfactual experiments discussed in Section 4.6. Figure 16 shows the resulting distributions of the ELB duration for all three learning models under the benchmark scenario with the estimated gain values, along with the average transition probabilities from ELB to the normal regime. This figure already reveals a large heterogeneity across the learning models: the AR(1) and LIL models generate a sizeable fraction of simulations that are still at the ELB after the 32 quarter period, with 25 % and 58 % respectively. Unlike these two models, the MSV-learning model leads to short-lived ELB episodes, with a majority of them lasting between 5 to 10 quarters. Looking at the average transition probabilities yields a similar pattern, with an exit probability of nearly 100 % for the MSV-learning model, 60 % for AR(1) and 40 % for LIL. The model with the largest estimated gain, i.e. LIL, yields the smallest exit probability, while the model with the smallest estimated gain, i.e. MSV-learning, yields the largest exit probability.

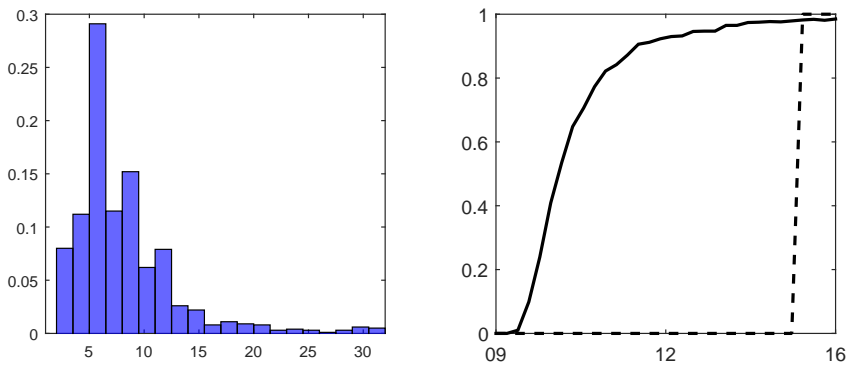
Figure 17 shows the average inflation and output growth from simulations over the counterfactual period for all models, which are in line with the ELB durations: the LIL model predicts a very large downside risk to both inflation and output growth, where a large number of simulations lead to deflationary spirals and falling output growth. For the AR(1) model, output growth evolves similar to the data. Simulated inflation values are typically lower than the data and the simulations indicate a downside risk, similar to the LIL model but smaller in magnitude. For the MSV model, both inflation and output growth are on par with the realized data and there is no downside risk in either process, unlike the AR(1) and LIL models. For the MSV model, the short ELB durations may seem at odds with the estimation results at a first glance. Given the small gain value, the simulations typically recover quickly before the learning dynamics build up a downward pressure. This is different than the estimation exercise, where the model is guaranteed to stay in the ELB regime long enough for the learning dynamics to kick in and reach sizeable effects. These results are consistent with the ELB frequency distributions discussed above, and they show that the prolonged ELB regimes in the AR(1) and LIL models are accompanied by below average output growth and inflation in the simulations.



(a) AR(1)

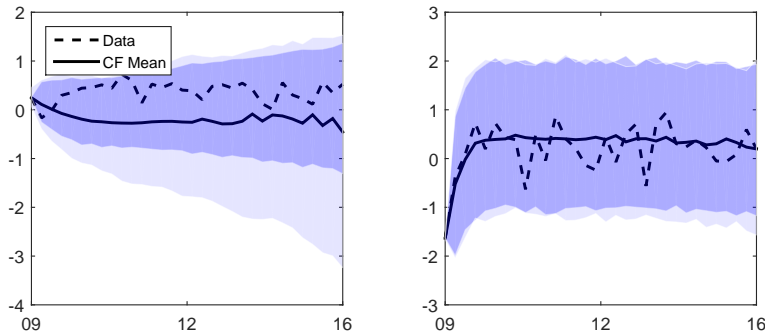


(b) LIL

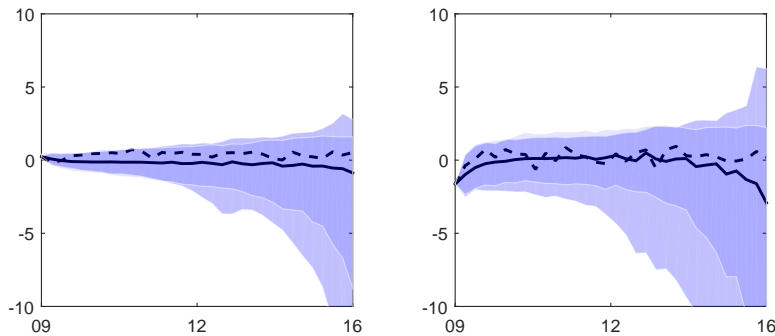


(c) MSV

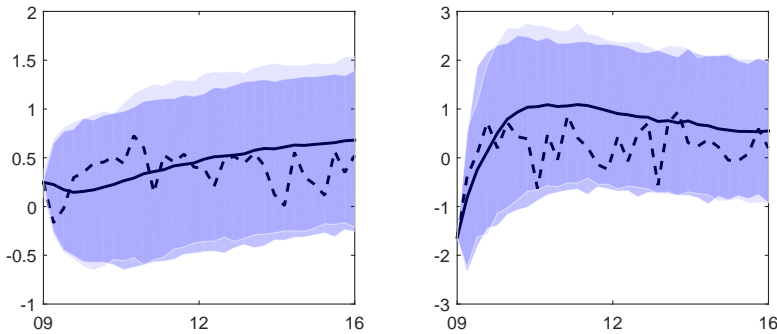
Figure 16: Left panel shows the distributions of the ELB duration for learning models. Right panel shows the average transition probabilities from ELB to the normal regime together with the estimated transition probabilities.



(a) AR(1) inflation and output growth



(b) LIL inflation and output growth



(c) MSV inflation and output growth

Figure 17: Monte Carlo distributions of inflation (left) and output growth (right) for the learning models over the counterfactual period. The dotted line shows the actual values of inflation and output growth, while the solid line shows the counterfactual mean. We plot two layers of uncertainty around the counterfactual mean: the inner layer shows the 90% interval from the MC experiment where the parameters are fixed at their posterior mean (hence the uncertainty is due to randomized shocks). The second layer shows the 90 % interval from the MC experiment where the parameters are drawn from their MCMC distribution at every simulation (hence the uncertainty interval is a combination of randomized shocks and parameter uncertainty).